ISTANBUL TECHNICAL UNIVERSITY ★ GRADUATE SCHOOL

MODELLING FORMATION OF FUEL-IN-OIL DUE TO POST INJECTIONS IN DIESEL APPLICATIONS

Ph.D. THESIS

Murat GÖNÜL

Department of Mechanical Engineering

Mechanical Engineering Programme

NOVEMBER 2021

ISTANBUL TECHNICAL UNIVERSITY ★ GRADUATE SCHOOL

MODELLING FORMATION OF FUEL-IN-OIL DUE TO POST INJECTIONS IN DIESEL APPLICATIONS

Ph.D. THESIS

Murat GÖNÜL
(503162015)

Department of Mechanical Engineering

Mechanical Engineering Programme

Thesis Advisor: Assoc.Prof. Dr.Osman A.KUTLAR

NOVEMBER 2021

İSTANBUL TEKNİK ÜNİVERSİTESİ ★ LİSANSÜSTÜ EĞİTİM ENSTİTÜSÜ

DİZEL MOTORLARDA ART PÜSKÜRTMELER SEBEBİYLE YAĞ SEYRELMESİ OLUŞUMUNUN MODELLENMESİ

DOKTORA TEZİ

Murat GÖNÜL
(503162015)

Makina Mühendisliği Anabilim Dalı

Makina Mühendisliği Programı

Tez Danışmanı: Doç. Dr. Osman A.KUTLAR

KASIM 2021

Murat Gönül, a Ph.D. student of İTU Graduate School student ID 503162015, successfully defended the thesis/dissertation entitled “MODELLING FORMATION OF FUEL-IN-OIL DUE TO POST INJECTIONS IN DIESEL APPLICATIONS”, which he prepared after fulfilling the requirements specified in the associated legislations, before the jury whose signatures are below.

Thesis Advisor :	**Assoc. Prof. Dr. Osman A. KUTLAR** İstanbul Technical University	.....
Jury Members :	**Asst. Prof. Dr. Alper T. ÇALIK** Istanbul Technical University	.....
	Asst. Prof. Dr. Hikmet ARSLAN Istanbul Technical University	.....
	Assoc. Prof. Dr. Orkun ÖZENER Yıldız Technical University	.....
	Prof. Dr. Muammer ÖZKAN Yıldız Technical University	.....

Date of Submission : 18 October 2021
Date of Defense : 26 November 2021

To my dear spouse, mother and grandmother,

FOREWORD

I would like to thank my thesis advisor Assoc. Prof. Dr. Osman A. KUTLAR for endless tehnical and emotional support. I also would like to thank Dr. Deniz Ş. YILDIZ for editing text during paper submission. I thank to Dr. Selmi Erim BOZDAĞ from Koç University Chemical Engineering Department for GC & FID oil sample measurements and to Ersin ALTIN and Azat ÇAKAN for supporting dyno tests and sample collection.

November 2021

Murat GÖNÜL
(M.Sc.)

TABLE OF CONTENTS

Page

ABBREVIATIONS

ASTM	**:** American Society for Testing and Materials
aTDC	**:** After Top Dead Center
CI	**:** Compression Ignition
CRA	**:** Crank Angle
DPF	**:** Diesel Particulate Filter
DI	**:** Direct Injection
DOC	**:** Diesel Oxidation Catalyst
ECU	**:** Engine Control Unit
EGR	**:** Exhaust Gas Recirculation
FID	**:** Flame Ionized Detector
GC	**:** Gas Chromotography
GPR	**:** Gaussian Process Regression
SCR	**:** Selective Catalytic Reduction
SE	**:** Squared Exponential
WLTP	**:** World Harmonized Light Duty Vehicle Test Procedure

SYMBOLS

L/d	**:** Injector nozzle length to diameter ratio
$\boldsymbol{FiO_{final}}$	**:** Fuel in Oil Concentration (Final)
$\boldsymbol{FiO_{init}}$	**:** Fuel in Oil Concentration (Initial)
$\boldsymbol{C_1}$	**:** Heavy fraction of oil dilution
$\boldsymbol{C_2}$	**:** Recovery rate of the light and the medium fraction of oil dilution
$\boldsymbol{x_{32}}$	**:** Sauter mean diameter
$\Delta\boldsymbol{P}$	**:** Difference between rail pressure and in-cylinder pressure
$\boldsymbol{\rho_{air}}$	**:** Charge air density
$\boldsymbol{Q}$	**:** Fuel flow
$\boldsymbol{D}$	**:** Injector needle hole diameter
$\boldsymbol{\rho_{liq}}$	**:** Fuel density
$\boldsymbol{t_b}$	**:** Break-up time
$\boldsymbol{S}$	**:** Penetration depth
$\boldsymbol{t}$	**:** Injection duration
$\boldsymbol{k(x, x')}$	**:** Kernel function

LIST OF TABLES

Page

LIST OF FIGURES

Page

MODELLING FORMATION OF FUEL-IN-OIL DUE TO POST INJECTIONS IN DIESEL ENGINES

SUMMARY

Post injections are frequently used for different purposes in diesel engines. However, post injections with specific configurations can cause oil dilution due to fuel percolating through cylinder walls. The fuel addition to the oil can cause deterioration in engine oil properties, which may result in engine failure. Therefore, the fuel concentration in oil needs to be monitored, and configurations of post injections are required to be optimized against oil dilution.

Usage of post-injection can be grouped under three different purposes; regeneration of Diesel Particulate Filter (DPF), desulfation of Selective Catalytic Reaction (SCR) and heat management strategies.

There are different types of emission pollutants emitted from diesel engines to the environment, such as particulate matter, CO, NO_x etc. DPF is placed in exhaust after-treatment systems to filter particle emissions emitted by diesel engines. The particles collected by DPF can penetrate and fill the pores of the filter; hence exhaust backpressure of the filter can be increased over time. Increased exhaust backpressure can affect both fuel consumption and the durability of engine hardware. Therefore, DPF is needed to be frequently cleaned from the soot known as carbon-based structures in emitted particles from diesel engines. Two methods can be used to clean DPF from the soot; active and passive regeneration. Active regeneration strategies rely on the combustion of soot by O_2 at a temperature range of 520-650°C. Passive regeneration strategies focus on burning soot by NO_2 at a temperature range of 300-400°C. Passive regeneration strategies are mainly used for long-haul heavy-duty truck applications as long haul driving conditions can sustain stable exhaust temperature within the window of passive regeneration and high exhaust flow with relatively high NO_2 concentration. Active regeneration is the primary strategy for DPF cleaning in most diesel engine applications except long-haul heavy-duty trucks. The temperature range of active regeneration can not be achieved only with engine measures. An exothermic reaction at the DPF inlet is needed to generate additional heat to increase and maintain exhaust temperatures within the active regeneration temperature range. For this reason, a Diesel Oxidation Catalyst (DOC) is required to be placed before DPF. Post injections with various injection timings are used to pull DOC wall temperature above light-off temperature and supply hydrocarbons for exothermic reaction upon DOC surface. Hydrocarbons can also be supplied with an external injector rather than a late post-injection. However, this approach also brings hardware complexity, specific uniformity requirements and additional cost to the overall after-treatment system. In conclusion, active regeneration strategies by supplying hydrocarbons with late post-injection are the primary technology route for most cases.

SCR systems are mandatory to comply with NO_x legislations. Diesel fuel may contain 10-15ppm sulphur. The sulphur is poisonous to SCR catalysts, especially to Cu-based SCR. Cu-based SCR is one of the most used SCR catalyst technology due to its high

performance in cold conditions. Sulphur poisoning reduces the chemical activity of SCR catalysts, so overall NO_x conversion efficiency drops in time. Therefore, SCR catalysts must be cleaned from sulphur with a certain frequency in high exhaust gas temperature, including high hydrocarbon content. With current after-treatment strategies on the market, the desulfation frequency of SCR is mainly coupled with the DPF regeneration schedule. So, the active DPF regeneration strategy is enough for the desulfation of SCR. However, a secondary SCR must be placed as a first brick in exhaust after-treatment system layouts under the influence of recent emission legislation updates in addition to conventional after-treatment systems. As a result, close-coupled SCR requires a separate desulfation strategy than active DPF regeneration. Post injections can be used to maintain necessary conditions for desulfation of the additional SCR catalyst.

Heat up and heat maintenance strategies are essential to achieve ultra-low NO_x levels as low as 0.02 g/bph-hr. Post injection strategies coupled with a close-coupled DOC before the first SCR catalyst is one of the effective options. There are other options to the heat-up system in the cold phase, like electrically heated catalysts, but these strategies require additional electrical structures and cost. Nevertheless, post-injection strategies have certain advantages on heat-up and maintaining heat strategies in terms of hardware complexity and cost. In addition, post-injection strategies offer more effective heating with less CO_2 penality than the electrical heater.

As a consequence of the increasing necessity of post-injection in three explained conditions, there will be an enormous increase in usage of post-injection strategies with new legislation, and oil dilution caused by post injections will become an emerging problem for all truck manufacturers and a more complex problem to contain for light and medium-duty vehicle applications.

There are two main mechanisms which are controlling the rate of oil dilution due to post-injection. The first mechanism is that fuel going into the oil pan through cylinder walls due to fuel contact with the wall, and the second mechanism is that fuel vapour in the oil pan might be recovered if it reaches enough vapour pressure. The first mechanism is affected by engine design parameters such as fuel injectors, ring pack and bowl design and calibration strategies such as post-injection timing and quantity and other calibration parameters. The second mechanism is mainly controlled by system design parameters such as oil operating temperature and oil volume. There is also the influence of engine speed on oil recovery. The oil dilution rate can be defined as a balance between the first and second mechanisms. In this study, the effect of calibration parameters on the first mechanism is focused, so post-injection strategies were activated for all times during steady and transient tests. The impact of the second mechanism on oil dilution measurements is normalized based on test data. A recovery test without post injections is conducted to analyze the effect of the second mechanism.

Oil properties such as viscosity with increasing fuel in oil concentration can deteriorate. As a result of viscosity change, oil dilution has specific effects on engine oil pumps and other engine components lubricated with oil. Fuel in oil concentration limit is lower in heavy-duty vehicles than other applications since in-service conformity is exceptionally high in heavy-duty vehicles. Three locations are sensitive against excessive oil dilution: crank bearing, cylinder liner and turbine-compressor shaft bearing. Besides these critical regions, excessive fuel in oil can lead to the fuel-oil mixture reaching intake via blow-by. In such a case, the engine may face over speed risk. The engine can handle the deterioration in oil properties to a certain level. There

is a trade-off between oil dilution rate, maximum oil deterioration that can engine bear and oil interval demand.

Several different measurement techniques can be used to analyze fuel concentration in engine oil. These measurement methods can be divided into three groups. The first group of measurement methods includes comparing total hydrocarbon input and output at the system level. The second group aims to estimate the concentration of fuel in the oil sample by comparing the physical condition of the sample with the fresh sample. And finally, the third group can be sorted as measurement methods aiming to measure fuel concentration in oil samples directly. Gas Chromatography and Flame Ionized Detector (GC&FID) was used to measure fuel concentration in samples in this study. This method is under the third group of the measurement categories. The third measurement group offers the best practice in terms of accuracy among all three above mentioned options since the third group aims to measure fuel concentration directly. However, GC&FID requires 4-6 hours in total for testing and measurement. So online optimization based on the most accurate measurement method is not possible. Therefore, the modelling studies can compensate for the disadvantage of the third group of measurement methods.

A series of different tests are conducted. During these tests, 208 oil samples were analyzed in GC&FID. Firstly, steady-state testing in 56 different operating conditions is completed with 168 oil samples. As an intermediate step, the recovery of Fuel in oil is characterized in the second test with 10 oil samples. In the final testing activity, 10 set of transient cycles in 5 different traces are completed with 30 additional oil samples. By these tests, the characterization of oil dilution mechanisms is aimed to be defined.

Possible input sets are determined based on a literature search and test data. The necessary input parameters are calculated in the Matlab Simulink environment. The correlation investigation is done with Python libraries. Finally, four modelling methods are applied, and the results are compared. The best input set and modelling approach indicated based on model results over transient test data.

DİZEL MOTORLARDA ART PÜSKÜRTMELER SEBEBİYLE YAĞ SEYRELMESİ OLUŞUMUNUN MODELLENMESİ

ÖZET

Dizel motorlarda art püskürtmeler sıklıkla kullanılmaktadır. Belirli koşullarda yapılan art püskürtmeler silindir duvarı üzerinden yağ ve yakıt karışımı şeklinde süzülerek yağ seyrelmesine sebep olabilmektedir. Yağdaki artan yakıt konsantrasyonu yağın özelliklerinde motorun zarar görmesine sebep olabilecek bozulmalara sebep olabilir. Bu sebeple, yağ içerisindeki yakıt konsantrasyonu sürekli olarak takip edilmelidir ve art püskürtmelerin zamanlamaları ve miktarları yağa giden yakıt miktarını en aza indirilecek şekilde optimize edilmelidir.

Art püskürtmelerin kullanım sebepleri üç grupta toplanabilir; DPF'in temizlenmesi, SCR'ın temizlenmesi ve termal yönetim stratejileri.

Dizel motorların çevreye saldığı kurum, CO, NO_x gibi pek çok zararlı madde vardır. Dizel motorların çevreye saldığı kurumu filtreleyebilmek için DPF kullanılmaktadır. Kurum DPF'in içerisine dolarak boşluklu yapısını tamamen doldurmaktadır, bunun sonucu olarak egzoz sisteminin toplam geri basınçı artış göstermektedir. Yükselen egzoz geri basıncının sonucu olarak yakıt tüketimi kötü etkilenmektedir ve hatta egzoz geri basıncının aşırı artışı motor parçaları bakımından dayanım problemleri oluşturabilmektedir. Egzoz geri basınç artışını düşürebilmek için belirli aralıkla DPF üzerinde biriken kurum temizlenmelidir. Bu temizleme işlemi için iki farklı strateji vardır, aktif ve pasif DPF temizleme işlemleri. Aktif DPF temizleme işlemi kurumun oksijen ile 520-650°C aralığında yanma reaksiyonu sonucu temizlenmesine hedeflemektedir. Pasif DPF temizle işlemi ise aktif DPF temizleme işleminden farklı olarak kurumun azotdioksit ile 300-400°C aralığında yanma reaksiyonunu kullanmaktadır. Pasif DPF temizleme stratejileri sıklıkla uzun yol kamyonları için terchi edilen bir DPF temizleme yöntemidir. Uzun yol kamyonları pasif DPF temizleme işlemi için gereken sıcaklık aralığında ve nispeten yüksek azotdioksit şartlarında stabil ve uzun süre çalışmaktadır. Aktif DPF temizleme işlemi uzun yol kamyonları hariç pek çok dizel uygulaması için ana akım olarak kullanılmaktadır. Aktif DPF temizleme işlemi için gerekli olan egzoz gaz sıcaklıkları sadece motor aksiyonları ile sağlanması ve kontrol edilmesi mümkün olmayacaktır. Dolayısıyla DPF girişinde ek ısı üretimi için ekzotermik reaksiyon ihtiyacı vardır. Bu sebeple DPF girişine DOC konumlandırılmaktadır. Farklı zamanlamalardaki art püskürtmeler ile DOC duvar sıcaklığı aktivasyon sıcaklığı üzerine taşınmakta ve DOC yüzeyinde ekzotermik reaksiyon için hidrokarbon tedariği sağlanmaktadır. Hidrokarbon tedariği iki farklı yöntemle sağlanabilmektedir. Egzoz hattı üzerine yerleştirilen ek bir yakıt enjektörü veya üst ölü noktadan uzakta yapılan art püskürtmeler yardımıyla hidrokarbon tedariği sağlanabilmektedir. Art püskürtmeler çoğu zaman tercih edilen hidrokarbon tedariği yöntemidir. Bu yöntem ile sisteme ek bir donanım eklemeden hidrokarbon tedariği mümkündür.

SCR sistemleri 2015 yılından beri neredeyse mecburi olarak dizel motor uygulamalarında atmosfere zararlı olan NO_x molekülünü indirgemek için kullanılmaktadır. Dizel yakıt 10-15ppm aralığında sülfür içerebilmektedir, sülfür bakır bazlı SCR katalistlerine karşı zehirlidir. Zehirlenme sonucu olarak SCR katalistlerinin kimyasal aktivitesi azalır, dolayısıyla SCR sisteminin yüksek verimle çalışmaya devam edebilmesi için SCR katalistlerinin zaman zaman sülfürden temizlenmesi gerekmektedir. SCR katalistlerinin yüksek sıcaklıkta ve ortamda hidrokarbon varken sülfürden efektif şekilde temizlenebilmektedir. Emisyon standartlarıyla birlikte konvansiyonel emisyon sistemlerine ek olarak fazladan bir adet daha SCR katalisti gereksinimi oluşmuştur. Bu ek SCR katalisti ısıl ataletten etkilenmemek için motora yakın konumlandırılmalıdır. Bu yeni konumu gereği SCR katalistinin sülfürden temizlenmesi aktif DPF temizleme işlemiyle birlikte yapılamayacaktır, dolayısıyla bu konumdaki SCR katalistinin sülfür temizliği için aktif DPF temizliğinden bağımsız bir stratejiye ihtiyacı vardır. Art püskürtmeler SCR sülfür temizliğindeki gerekli şartların sağlanmasında önemli bir yöntemdir.

Isıtma ve sıcaklık kontrol stratejileri aşırı düşük NO_x başarımları için oldukça önemlidir. Egzoz sistemindeki ilk katalistin DOC olması durumunda art püskürtmeler ısıtma ve sıcaklık kontrol stratejilerinde avantajlı bir yere sahiptir. Isıtma ve sıcaklık kontrolü için elektrikli ısıtılan katalistlier gibi farklı stratejiler mümkündür. Fakat bu stratejiler ek elektriksel bağlantılar ve maliyet getirmektedir. Bu noktada art püskürtmeler parça kompleksitesi ve maliyet açısından avantaja sahip oldukları için sıklıkla kullanılmaktadır. Ek olarak yakıt tüketimi açısından art püskürtmeler elektrikli ısıtıcılardan daha efektiflerdir.

Art püskürtmelerin kullanım alanları üç ana kategoride açıklanmıştır. Bu kullanım alanlarında yeni gelen emisyon regülasyonları sebebiyle artış beklenmektedir. Art püskürtmelere olan ihtiyacın artmasıyla birlikte art püskürtmelerdan kaynaklanan yağ seyrelmesi ağır ticari araçlar için yeni ve hafif/orta ticari araçlar içinde çözülmesi daha zor olan bir problem haline gelmektedir.

Yağ ile yakıtın birbiriyle olan etkileşim mekanizmaları incelendiğinde iki temel mekanizmadan söz etmek mümkündür. İlk mekanizma yapılan art püskürtmenin silindir duvarı ile teması sonrasında piston haraketiyle silindir duvarındaki yağ ve yakıt karışımının yağ karterine süzülmesi olarak tanımlanabilinir. Bu mekanizmaya yanma sırasındaki silindir içerisindeki basınçlı hava-yakıt karışımının sekmanlar aracılığıyla kartere ulaşması da dahil edilebilinir. Yağ karteri içerisindeki yakıt, yağ çalışma sıcaklığına bağlı olarak yanma odasına geri dönmektedir. Bu geri dönüşüm mekanızması da ikinci temel mekanizma olarak ifade edilebilinir. İlk mekanizma yakıt enjektörü geometrisi, sızdırmazlık elemanlarının durumu ve yanma odası tasarımı gibi değişkenlerden etkilenebildiği gibi ray basıncı, art püskürtme miktarı ve zamanlaması gibi çeşitli kalibrasyon parametrelerinden de etkilenebilmektedir. İkinci mekanizma daha ziyade yağ çalışma sıcaklığı ve yağ hacmi gibi sistem tasarım parametrelerinden etkilenmektedir. Motor devri her iki mekanizma üzerinde de etkilidir. Bu çalışmada ilk mekanizmanın üzerindeki kalibrasyon parametrelerinin etkisi incelenecektir, bu sebeple tüm çalışma boyunca art püskürtmeler aktif edilmiştir. İkinci tanımlanan mekanizmanın karekterizasyonu içinde ek test yapılmıştır ve art püskürtme olmaksızın tamamlanmıştır.

Viskozite gibi yağ özellikleri artan yağdaki yakıt konstrasyonuyla birlikte bozulabilmektedir. Viskozite değişiminin sonucu olarak yağ pompası ve farklı motor parçaları zarar görebilmektedir. Ağır ticari araçlar yağ özelliklerinde bozulmalara hafif

ve orta ticari araçlara kıyasla, kullanım ömürleri oldukça uzun olması sebebiyle, daha hassastır. Yağ özelliklerinin değişiminden etkilenen üç temel bölge vardır; krank şaft yatakları, silindir içi duvarları ve türbin-kompresör arasındaki şaft olarak sıralanabilinir. Yağdaki yakıt konstantrasyonun artmasıyla birlikte karterdeki yağ ve yakıt karışımı hacmi artış göstermektedir. Eğer yağdaki yakıt konstrasyonu kontrol edilmez ve aşırı yükselirse, hava yoluna yağ-yakıt karışımı ulaşabilir ve motoru aşırı yüksek devre zorlayıp, zarar görmesine sebep olabilir. Yağ özelliklerindeki bozulma motor dayanımı açısından belirli bir noktaya kadar sorun oluşturmayabilir fakat yağ seyrelmesi şiddeti, motorun dayanabileceği maksimum yağ bozulması ve müşterinin yağ değişim aralığı isteği arasında bir denge kurulması gereklidir. Bu dengede doğru yerde konumlanabilmek için yağ seyrelmesinin modellenmesi gerekmektedir.

Yağın içerisindeki yakıt konsantrasyonunu ölçmek için farklı teknikler mevcuttur. Bu teknikleri genel olarak üç gruba ayırabiliriz. Birinci grup olarak yağa giden yakıt miktarının anlık olarak ölçülmesinin hedeflendiği metodlardan bahsedilebilinir. Bu metodlarda egzoz gazı içerisindeki toplam karbon konstantrasyonu ölçülmektedir, egzoz gazı debisi de kullanılarak sistemden atılan toplam karbon miktarı hesaplanmaktadır. Sistemden atılan toplam karbon miktarı yakıt debisi ölçüm cihazı ile karşılaştırılarak aradaki anlık fark yağa giden yakıt miktarı olarak hesaplanmaktadır. Bu metod ile teoride karşılaştırılabilinir sonuçlar elde edilebilinir fakat uygulamada bu yöntemin ihtiyaç duyduğu üç alt ölçüm cihazının ölçüm hassasiyetini sürekli olarak aynı noktada tutmak mümkün değildir. İkinci ölçüm metodu olarak yağın içerisindeki yakıt miktarının dolaylı olarak ölçüldüğü yöntemler belirtilebilinir. Yağın kinematic viskozitesinin değişimi üzerinden yağın içerisindeki yakıtın konsantrasyonun hesaplanması bu yönteme girmektedir. Fakat yağın özelliklerini etkileyecek tek parameter yağ seyrelmesi olmayacağı için bu metod ile yapılan analizlerin sonuçları sadece belirli şartlar altında doğru olacaktır. Üçüncü metod ile yağ içerisindeki yakıt miktarının direk ölçümü yöntemidir. Bu yöntem için GC & FID kullanılmaktadır, dolayısıyla yağın içerisindeki tüm yakıt molekülleri teker teker buharlaştırılarak ölçülmektedir. Bu yöntemde ölçümün yapılabilmesi için yağ içerisindeki yakıt konsantrasyonunun yükselmesi gerekmektedir. Dolayısıyla, sabit şart altında yağ seyrelmesinin şiddetinin tek bir çalışma noktasında ölçülebilmesi için 4-6 saat test edilmesi gereklidir. Bu süre aralığı düşünüldüğünde bu ölçüm yöntemine göre anlık olarak art püskürtme stratejilerinin optimizasyonu mümkün olmayacaktır.

Yağa süzülen yakıt miktarının karekterizasyonu için tez kapsamında pek çok aşamalı motor testleri yapılmıştır. Bu testler sırasında toplam 208 adet numune GC & FID metoduna göre analiz edilmiştir. Duragan testlerde 56 farklı çalışma noktasında toplam 168 örnek toplanmıştır. Ara bir adım olarak, yağın içerisindeki yakıtın geri dönüşünün karekterizasyonu için 10 numune daha ayrı bir test sırasında alınmıştır. Tez kapsamında son test çalışması olarak 5 farklı hız profilinde yağ seyrelmesi test edilmiştir, bu test sırasında da 30 ek numune daha alımıştır.

Yağ seyrelmesi şiddeti ile korelasyonu olabilecek parametreler literatür araştırması ve makine öğrenmesi yöntemleriyle belirlenmiştir. Parameterlerin hesaplanması Matlab Simulink ortamında yapılmıştır. Korelasyon ve modelle çalışmaları Python ortamında pek çok kütüphane kullanılarak yapıldı. İki farklı modelleme metodu duragan test sonuçlarına uygulanarak, modelleme yöntemleri yağ seyrelmesi problemi için birbirleriyle kıyaslanmıştır.

Yapılan çalışmaların sonucu olarak, yakıt sebebiyle oluşan yağ seyrelmesinin motor kalibrasyon parametrelerine duyarlı şekilde modellenmesi başarılmıştır. Tezde

tanımlanan modelleme metoduyla, aktif DPF rejenerasyon motor kalibrasyonun yağ seyrelmesi açısından incelenmesi mümkündür. Dolayısıyla kalibrasyon geliştirme sürecinde gerçekleştirilen bazı tekrarlı adımların iyileştirilmesi ve toplam ürün geliştirme maliyetinin azaltılması mümkündür.

1. INTRODUCTION

1.1 Purpose of Thesis

In recent years, environmental issues have become a more and more concerning problem worldwide. A series of emission standards are mandated almost all around the world to reduce pollutants and greenhouse gases. Different standards and laws define levels of pollutant emissions that engine manufacturers must obey. Consequently, engine manufacturers design new technologies for achieving emission reductions.

Leading technologies for gasoline engines to fulfil the exhaust emission levels have been implemented, such as downsizing, gasoline particulate filter and turbocharging. Meanwhile, diesel engines require more complex efforts. In emission reduction, engine manufacturers have different approaches in the gas exchange process, injection systems and after-treatment systems.

Standard after-treatment system devices for emission legislation in diesel applications that is newer than 2016 are exhaust gases recirculation (EGR), diesel particulate filter (DPF) and selective catalysts systems, also known as SCR (Selective Catalytic Reduction). In Figure 1.1, emission limits for different emission legislations are given. N_2O and CH_4 are known pollutants and will be most probably limited with Eu7 and later. The limit for these pollutants is still under discussion since Eu7 has not been entirely determined yet. It is certain that NO_x limitation with Eu7 will drop. However, the exact limit is still under discussion. Therefore, the numbers discussed are changing between 0.03-0.15g/kWh. Considering that the new limit will dramatically drop from the Eu6 limit, more complex and challenging after-treatment systems are expected to be introduced to the market.

Stage	Year	Test	CO	HC	NOx	PM	N2O	CH4	PN
			g/kWh						1/kWh
Euro I	1992	ECE	4.5	1.1	8	0.36			
Euro II	1996	ECE	4	1.1	7	0.25			
Euro III	2000	ESC & ELR	2.1	0.66	5	0.1			
Euro IV	2005	ESC & ELR	1.5	0.46	3.5	0.02			
Euro V	2008	ESC & ELR	1.5	0.46	2	0.02			
Euro VI	2013	WHTC & WHSC & PEMS	1.5	0.13	0.4	0.01			8.00E+11
Euro VII	2025	WHTC & WHSC & PEMS	1.5	0.13	0.1		?	?	8.00E+11

Figure 1.1 : Emission standards for different emission levels [1].

The EGR is used for the reduction of nitrogen oxides (NO_x) emissions in diesel engines. This process includes recirculating a portion of exhaust gases to the intake system to mix fresh air with exhaust gases to reduce the maximum combustion temperatures. Lower combustion temperatures avoid the generation of NO_x regarding Zeldovich NO_x formation mechanism. Yet, increased exhaust gases in the intake can boost soot formation and increase the appearance of other pollutants. The Diesel Particulate Filter (DPF) aims to physically capture soot inside and on filter walls to comply with particulate emission limits. In Figure 1.2, soot capturing through DPF channels is illustrated.

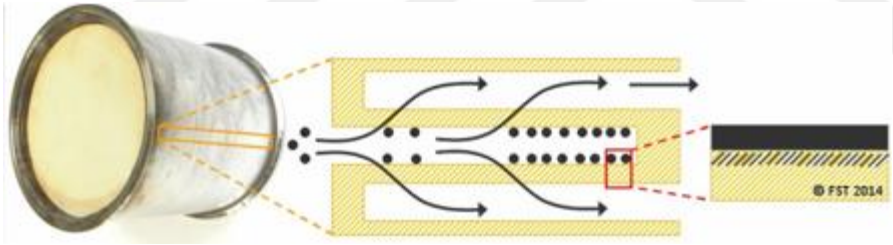

Figure 1.2 : DPF capturing soot particles.

With the increasing amount of soot captured inside and on DPF walls, backpressure over the filter is increased. Therefore, DPF is required to be frequently cleaned from the soot. There are two main approaches to clean DPF from soot; active and passive regeneration. Passive regeneration means that soot trapped inside the filter is burned by NO_2 in temperatures within the range of 300-400°C. [2]

Passive Regeneration

$C + 2NO_2 \rightarrow CO_2 + 2NO$

$C + NO_2 \rightarrow CO + NO$

Figure 1.3 : Passive soot burn chemical equations [3].

This strategy requires a relatively long steady drive compared to the active regeneration strategy. As a result, usage of only passive regeneration strategy is quite limited to long haul trucks. Mostly, passive regeneration strategy is coupled with active regeneration for system safety. Active regeneration relies on the combustion of soot by O_2 in the temperature range of 520-650°C. Such a high-temperature range can be sustained with post-injection strategies.

Active Regeneration

$C + O_2 \rightarrow CO_2$

$C + \frac{1}{2}O_2 \rightarrow CO$

Figure 1.4 : Active soot burn chemical equations [3].

The purpose of selective catalyst systems is converting NO_x emission with the aid of diesel exhaust fluid (DEF) into diatomic nitrogen (N_2), water (H_2O) and a small amount of carbon dioxide (CO_2). DEF is a reducing agent which can be anhydrous ammonia, aqueous ammonia or urea.

$4NH_3^{\vartheta} + 4NO + O_2 \rightarrow 4N_2 + 6H_2O$	Standard SCR Reaction
$4NH_3^{\vartheta} + 2NO + 2NO_2 \rightarrow 4N_2 + 6H_2O$	Fast SCR Reaction
$4NH_3^{\vartheta} + 3NO_2 \rightarrow 3.5N_2 + 6H_2O$	NO_2 SCR Reaction

Figure 1.5 : SCR chemical reactions [3].

Although these after-treatment measures can effectively reduce tailpipe emissions below regulated limit, they also compromise certain aspects of engine oil [4]. Due to increased usage of EGR to achieve lower NO_x emissions, soot generation, is increased. While part of the soot generation will be expelled with exhaust gases from the combustion chamber, a portion of generated soot can impinge on the oil film of the cylinder wall. And, these impinged soot particles can pass to engine oil through rings. As a result of soot additive on bulk oil, tribo-chemical properties of the engine may change. As it interferes with the additives and depletes them, increased soot concentration in engine oil restricts the generation of tribofilm.

Furthermore, DPF regeneration frequencies are increasing due to increased soot generation due to higher EGR rate usage to comply with low NOx emission limits. Post-injections are essential for the process of active regeneration. The purpose of these post-injections can be sorted into two categories [5]. First, the active regeneration process requires sustaining exhaust temperature at the range of 520-650°C. This temperature range is not achievable with only engine measures. So, an exothermic reaction on after treatment system components to achieve these high temperatures is required. Diesel Oxidation Catalyst (DOC) is located upstream of DPF with the purpose of exotherm generation. The purpose of the first category of post-injections can be given as hydrocarbon (HC) suppling to DOC so exothermic reaction on the surface of DOC can occur. As most of the catalysts require a specific temperature for activation, called light-off temperature, engine out temperature is needed to be elevated and maintained at 300°C for activation of DOC. The second purpose for post-injections is to increase the engine out gas temperature to reach up to DOC light-off temperature and sustain exhaust gas temperature above DOC light-off temperature all the time. Depending on the configuration of post-injections, a portion of the post-injection can not be burnt inside the combustion chamber. When fuel droplets are condensed on the surface of combustion chamber walls, fuel can pass through the ring pack and mix with the engine oil.

One of the significant problems with oil dilution due to fuel addition is that fuel concentration in the oil speeds up the breakdown of lubricants. The fuel content in engine oil decreases engine oil viscosity, resulting in a higher risk of contact between metal surfaces and the lubricated engine components. Moreover, engine oil consumption due to lowered oil viscosity can increase.

In summary, the emission control strategies can provoke and accelerate oil degradation by contamination of both soot and fuel. With narrowing pollutant limits, the usage of emission control strategies is widely extended. And, contamination of engine oil due to emission control strategies is becoming an emerging problem. Therefore, a series of tests are conducted to understand the formation of oil dilution due to fuel addition in this study. With this study, the effect of DPF active regeneration with post-injections on engine oil is investigated. In the light of conducted test results, the relation between engine control parameters and oil dilution mechanisms are comprehensively given.

1.2 Literature Review

Because of the increasing necessity of post-injection in explained conditions, there will be an enormous increase in usage of post-injection strategies with new legislation, and oil dilution caused by post injections will become an emerging problem for all truck manufacturers and a more challenging problem to overcome for light and medium-duty vehicle manufacturers. There are several effects of increasing fuel concentration in engine oil. Studies by Wattrus et al. [6] have shown oil properties can deteriorate with fuel contamination. For example, 50% kinematic viscosity reduction was reported in 15% fuel in oil concentration.

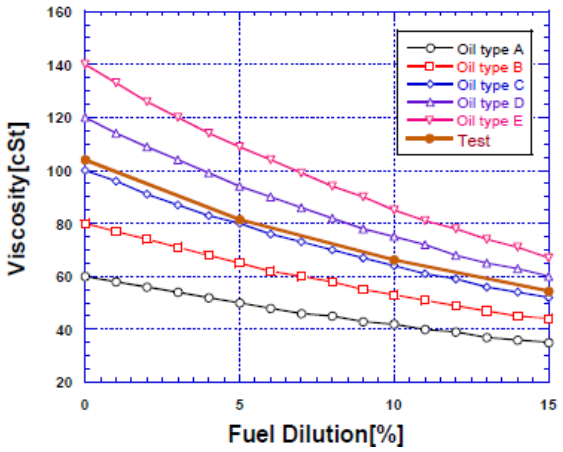

Figure 1.6 : Viscosity reduction as a function of oil dilution [6].

Motamen et al. [7] studied the effect of oil dilution on the engine oil pump. The excessive fuel addition to the engine oil could represent a drop in oil pressure, weakness in lubricant detergency, acceleration in lubrication oxidation, formation of varnish, and some acid. Studies by Penchaliah et al. [8] indicated that wear rate was mainly influenced by acid and soot additions, while all contaminants and contaminant levels increased the coefficient of friction. Therefore, fuel contamination promotes oil oxidation, creates some acid that might result in a wear rate increase, and increases fuel consumption by increasing the coefficient of friction. In addition to that, fuel contamination contributes to the toxic and hazardous characteristics of motor oil waste.

In another aspect, fuel addition to oil can increase engine oil volume to a critical level. Above the critical level, oil and fuel mixture cannot be appropriately circulated; thus, oil and fuel mixture can be introduced to engine combustion through the air path. Combusting engine oil and fuel mixture in the cylinder can cause more severe engine

and after-treatment systems damage by increasing combustion gas temperatures excessively and promoting ash generation.

The studies have shown that oil dilution rate was affected by several parameters such as engine design, oil/fuel type, and engine calibration. Previous studies by Shibata et al. [9] and Fansler et al. [10] have shown that the fuel addition mechanism can be explained by liquid fuel impingement on lubricated cylinder walls and the adsorption of fuel into the oil film. The oil film on the cylinder liner is maintained by piston motion. The reciprocating motion of a piston has new oil from the sump supplied to the liner, and the previous oil having a fuel component returned to the sump in terms of scraping down the oil film. Oil dilution also occurs while the blow-by gas is passing through the ring pack of a piston. In studies from Artmann et al. [11], rail pressure, post quantity and timing were investigated and indicated as effective parameters on oil dilution rate.

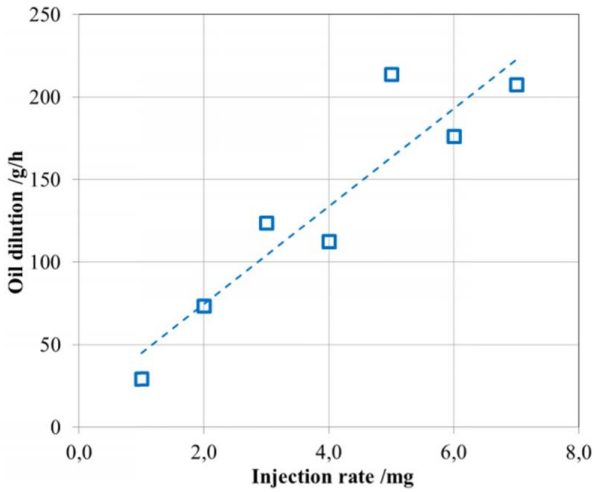

Figure 1.7 : Oil dilution formation vs post-injection quantity [11].

Different post-injection quantities under the same conditions were investigated. As a result, a linear relationship between the post-injection amount and oil dilution formation rate was observed by Artmann et.al.[11].

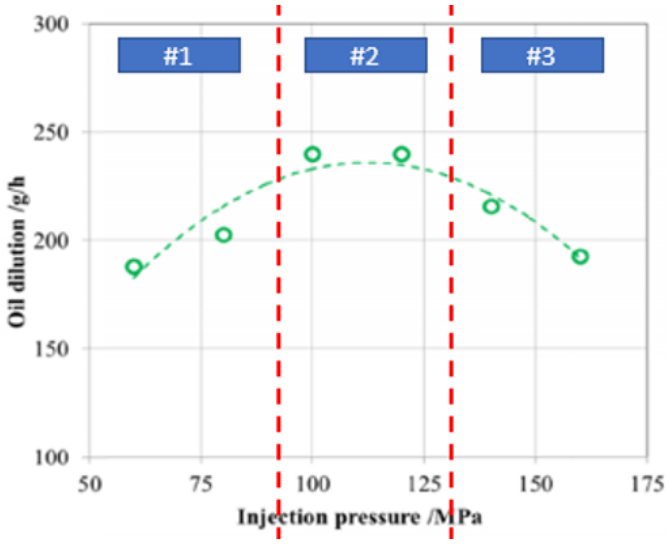

Figure 1.8 : Oil dilution formation vs post-injection pressure [11].

When rail pressure was the only swept parameter, It can be seen in the Figure 1.8 that rail pressure had a specific influence on oil dilution formation rate. As rail pressure was relatively low in section #1, the momentum of fuel spray was minimal. As a result, fuel spray and cylinder wall interaction was minimal. Thus, the oil dilution formation rate was relatively low. In section #2, the momentum of fuel spray was somewhat higher, yet the atomization regime did not take place. Therefore, the oil dilution formation rate reached its maximum. In last section #3, the atomization regime took place, and spray penetration dropped. As a result, a decrease in oil dilution formation rate was observed. In conclusion, there is a dependency of rail pressure on oil dilution formation rate.

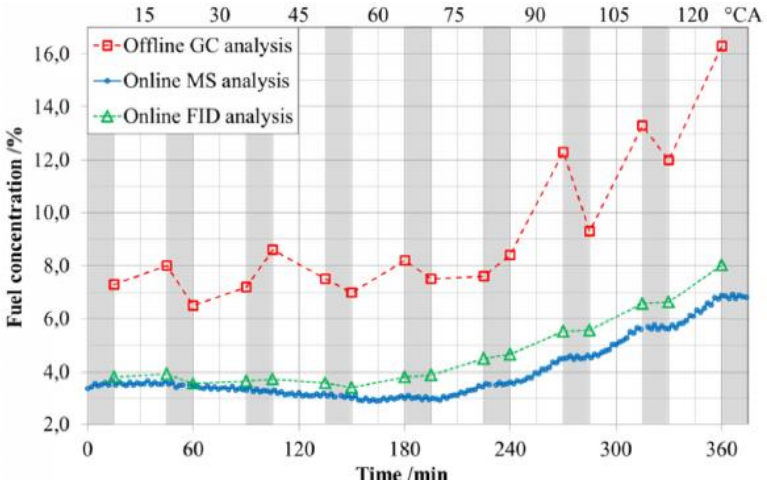

Figure 1.9 : Oil dilution formation vs post-injection timing [11].

A test was conducted with different start of injection timings with the presence and absence of post-injections, as shown in Figure 1.9. In the test, the white zone indicates that post-injection was present during testing. Contrary, the grey area means that post-injection was off during testing in that specific zone. Several measurement techniques are shown on the graph, yet offline results are the most reliable among all three. Based on the offline analysis in white zones, it can be seen that if post-injection was retarded more, the increase of fuel concentration for the same duration of testing was increased. This is basically because of decreased in-cylinder pressure and parallel to that decreased in-cylinder gas density that fuel spray going into with retarded injection timing. Therefore, post-injection timing was observed as one of the effective parameters over oil dilution.

Kidoguchi et al. [12] studied different piston geometries and showed that piston geometry affects oil dilution formation. Studies by Hulkkonen et al. [13] have demonstrated the influence of different fuel types on oil dilution. Studies by Artmann et al. [11] also showed that lower coolant temperature could promote the formation of oil dilution.

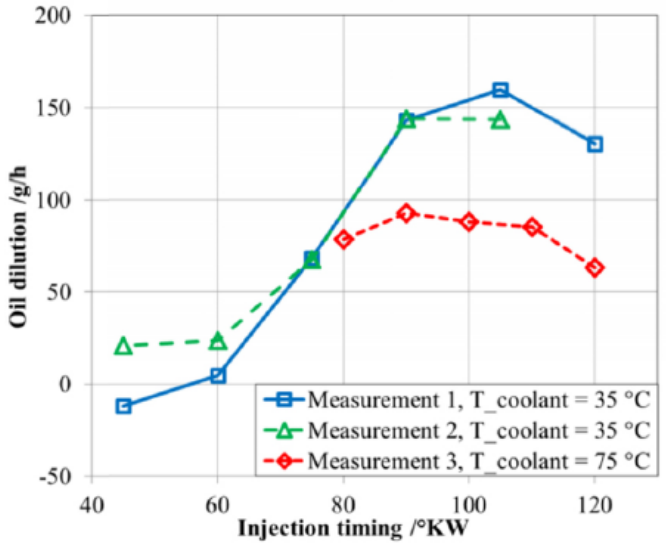

Figure 1.10 : Oil dilution formation vs coolant temperature [11].

In Figure 1.10, Measurement 1 and Measurement 2 were recorded in the same coolant temperature. The deviation between these two measurements was only coming from test deviations. The difference between these two measurements and Measurement 3 indicated the effect of coolant temperature over oil dilution formation.

The fuel added to the engine oil can also be evaporated, and the evaporation of the fuel from the engine oil is called oil recovery. The fuel recovery mechanism is primarily controlled by oil operating temperature and fuel molecule concentrations in engine oil. The vapour pressure of each carbon molecule is different in constant oil temperature based on the length of the carbon chain. Long chained carbon molecules, which are very close to carbon structure in oil, create less vapour pressure in oil operating temperatures, so this portion of the fuel in oil cannot be recovered in practice. On the other hand, short-chained fuel molecules in oil have high vapour pressure in the oil operating temperature range. Therefore, this portion of the oil dilution is possible to be recovered. [11]. In Figure 1.11, long carbon chain molecules such as C_8H_{16} was not evaporated at all. On the contrary, molecules such as C_4H_{10}, C_5H_{10} and C_5H_{12} were evaporated. However, the rate of evaporation was observed to be dropping over time.

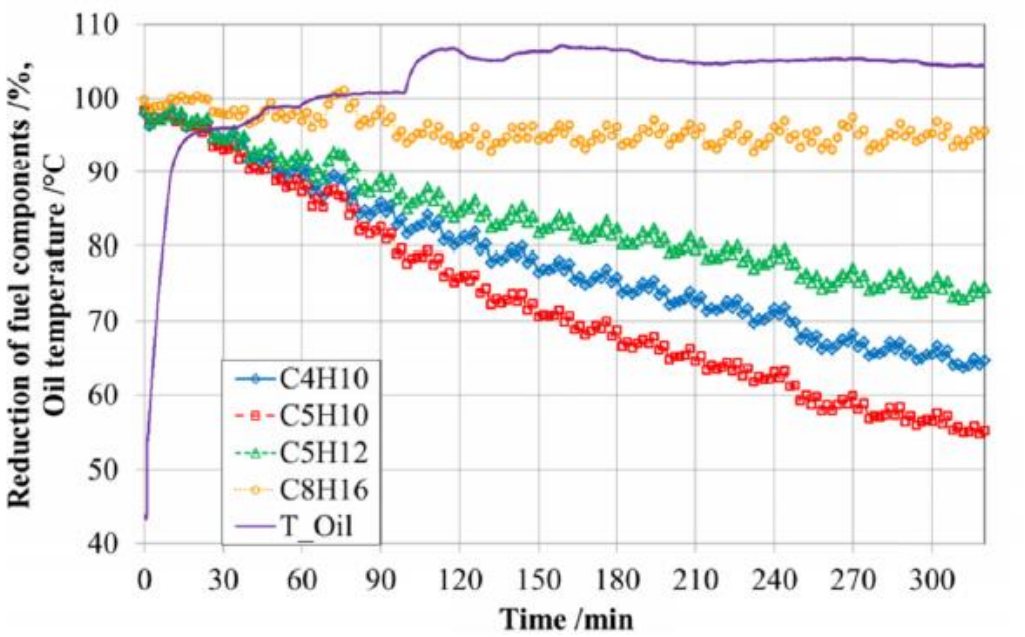

Figure 1.11 : Oil dilution recovery [11].

In studies by Wattrus, the correlation between SMD and oil dilution rate was shown. Therefore, the correlation between spray parameters and oil dilution was already investigated in the literature. However, the main objection was that the correlation could only exist when all spray parameters are considered simultaneously. The correlation between SMD and oil dilution rate only exists if spray penetration is not changing dramatically. Based on the test results obtained in our study, we also observed the correlation between SMD and oil dilution only when penetration depth

was kept constant. When both spray penetration depth and SMD change in different directions, a direct correlation between SMD and oil dilution rate is not possible.

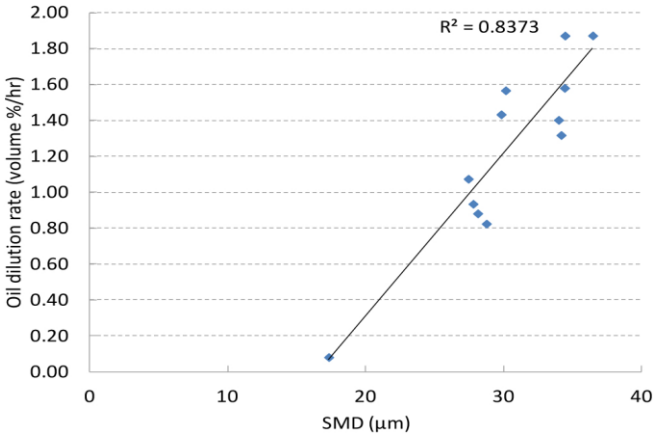

Figure 1.12 : Oil dilution formation vs SMD [6].

1.3 Hypothesis

There should be a correlation between parameters controlling fuel spray properties and the formation rate of oil dilution. If this correlation can be shown with empirical spray parameters, implementing a modelling approach based on this correlation into electronic control units (ECU) on vehicle applications would be possible. Furthermore, optimization of engine control parameters against oil dilution can be possible via this correlation.

2. TESTING DETAILS

2.1 Engine Details

There were three different sets of experiments conducted in this study to characterize oil dilution due to post injections. A steady-state test with deviations in control parameters such as rail pressure, post-injection quantity, and timing were completed in the first set of tests. The primary purpose of this test was to measure the change in the rate of fuel going into the oil pan within a specific period due to post injections in different configurations. During steady-state tests, 168 oil samples were collected. These oil sample results indicated the difference between fuel addition and removal from the oil pan. The fuel recovery rate was required to be determined to calculate gross oil dilution rate from steady-state test results. Therefore, the second test was conducted for the characterization of fuel recovery. 11 oil samples were collected in the fuel recovery characterization test. The third test was conducted to investigate the accuracy and behaviour of the modelling approach over transient conditions for different driving profiles under quasi-steady assumptions. 20 oil samples were collected during the transient tests over five different vehicle speed profiles representing various use cases.

Engine specifications are shown in Table 2.1. A 4-cylinder and 4-stroke compression-ignition (CI) light-duty Direct Injection (DI) engine was used during experiments. This engine was also equipped with a common-rail injection system and a turbocharged/intercooler air loop system. Although EGR was mounted on the engine, the EGR valve was shut off to not expose the EGR system with excessive hydrocarbon coming from the engine due to late post injections.

Table 2.1 : Engine specifications.

Parameter	Value
Engine Volume(L)	1.5
Numb.of Cylinders	4
Bore(mm)	73.5
Stroke(mm)	88.4
Oil Volume(L)	3.8
Oil Specification	SAE 5W-30 CJ-4
Compression Ratio	16
Numb.of Inj. Holes	8
Inj. Hole Dia(mm)	0.108
Inj. L/D Ratio	6.3

During the experiments, crude-oil based EN590 diesel with 5% of biofuel was used. EN590 is the European standard fuel. The fuel properties were shared in Table 2.2.

Table 2.2 : Fuel properties.

Property	Unit	Test Method	Measurement
Cetane number	-	EN ISO 5165	52.0
Density @15°C	kg/m³	EN ISO 12185	835.9
Viscosity @ 40°C	mm²/s	EN ISO 3104	3.8
Flash Point	°C	EN ISO 2719	66.0
Sulphur Content	mg/kg	EN ISO 20846	6.8

In-cylinder pressure was measured with AVL GH14P glow plug sensors and recorded with AVL INDISMART and Concerto interface. In-cylinder pressure was recorded at 30-60-90-125-160 CA aTDC. Engine control parameters are recorded with ATI Vision by direct connection to ECU. Engine coolant temperature was kept at 90°C with an external conditioner. The intention was to control oil temperature as well. However, adding an oil cooling system to the test bench increased the oil volume due to piping and increased testing duration. Therefore, the oil temperature was not directly controlled but kept within 90-95°C by conditioning coolant used in the oil heat exchanger at 90°C. Holding force at dynamometer was controlled with AVL electric dynamometer.

Figure 2.1 : Test engine before connecting to the dynamometer.

2.2 Steady State Tests

A relatively early close post-injection is mostly coupled with late post-injection in active regeneration strategies. Therefore, a combination of post injections was tested during steady-state tests. There is a pattern in the steady-state test matrix shown in Figure 2.2 and Figure 2.3. The pattern also enables the determination of the oil dilution rate for each post-injection separately. In every four test points, all of the parameters except post configuration were kept the same. The first test point was set to have only close post-injection in every group of four test points. The consecutive test points in the same group had second late post-injection with increasing quantity. Therefore, the contribution of the second post-injection was determined by the delta between the corresponding test point and the first test point in every group.

In every group of four test points, parameters such as speed, load, rail pressure, post-injection quantity and timing, air-to-fuel ratio were swept. Hence, different sprays and charge conditions were coupled to create an input set to the models in further studies. The details of the test matrix were shown in Figure 2.2 and Figure 2.3.

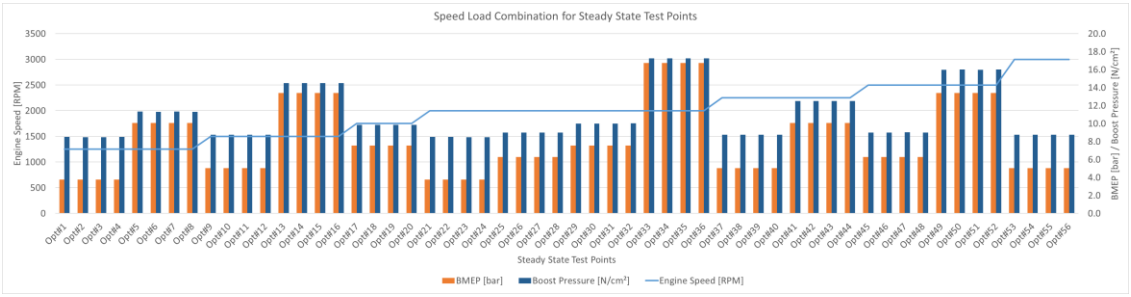

Figure 2.2 : Speed and load point for the steady-state test.

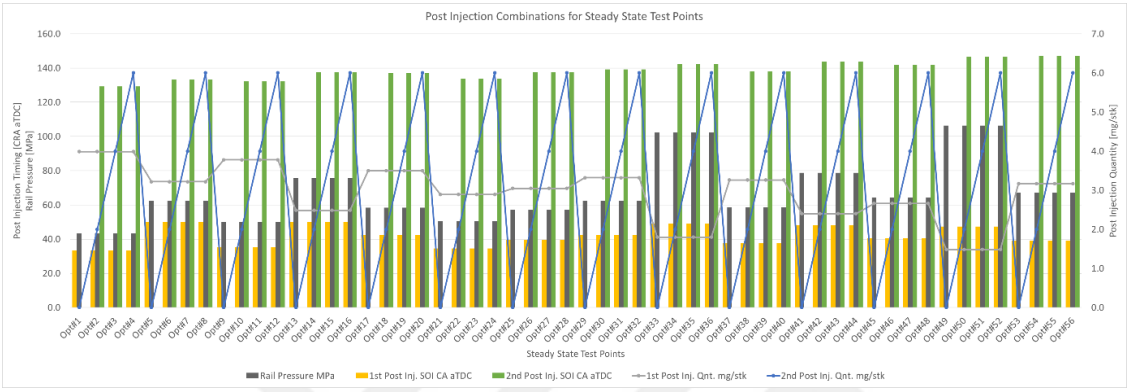

Figure 2.3 : Post and rail pressure parameters for the steady-state test.

Each test point shown in Figure 2.2 and Figure 2.3 was tested separately, and 3 samples were collected at each test point. Engine oil was always changed after the third sampling, and each first sample was collected from the oil pan after 15min of engine operation without post injections. Even though the oil and oil filter were changed at the beginning of each new test point, the first sample was always needed to measure leftover oil dilution in the system. Oil samples are taken from oil level indicator metallic housing with plastic pipe and syringe as shown in Figure 2.4. A new plastic pipe and syringe were used in each sampling. The oil sample was always taken from mixed oil. The samples in each test point are kept at three since collecting more samples can affect test results by changing oil volume. Test duration at each test point was adjusted based on the literature review. In high and late post-injection configurations such as Opt#4, testing duration kept low compared to Opt#1. The main reason for altering testing durations was to generate measurable fuel concentration in optimum testing duration. Therefore, the overall test duration was shortened. As fuel addition (gross or net) was calculated in ml/sec later, testing duration in each test point became irrelevant.

Figure 2.4 : Sampling from oil level indicator housing.

2.3 Recovery Tests

In addition to steady-state tests, a characterization test for the oil recovery pattern was conducted. The oil temperature was kept at 90-95 °C in parallel to steady-state tests. Hence, the oil recovery characterization obtained with this test could be used to revert the effect of oil recovery on steady-state tests. A combination of steady-state test points (Opt#4-26-40) was selected for oil dilution generation purposes based on steady-state test results. During the oil dilution generation phase, the test point was periodically changed between Opt#4-26-40. The oil dilution generation phase was completed in 6.5 hours. 4 samples were collected in the oil dilution generation phase. Like steady-state tests, the first sample was collected after oil was changed, and the engine was run for 15min without post injections. The oil dilution limit in light-duty applications is generally in the range of 10-15%. Therefore, the duration of the oil dilution generation phase was determined by aiming at that level. Recovery testing was done after steady-state testing. The duration of the oil dilution generation phase was determined based on steady-state test results. Once the oil dilution generation phase was completed, the WLTP trace kept running for 115 hours without any post injections in the evaporation phase. Thus, seven samples with uniform intervals were collected during the evaporation phase. The recovery test plan is illustrated in Figure 2.5.

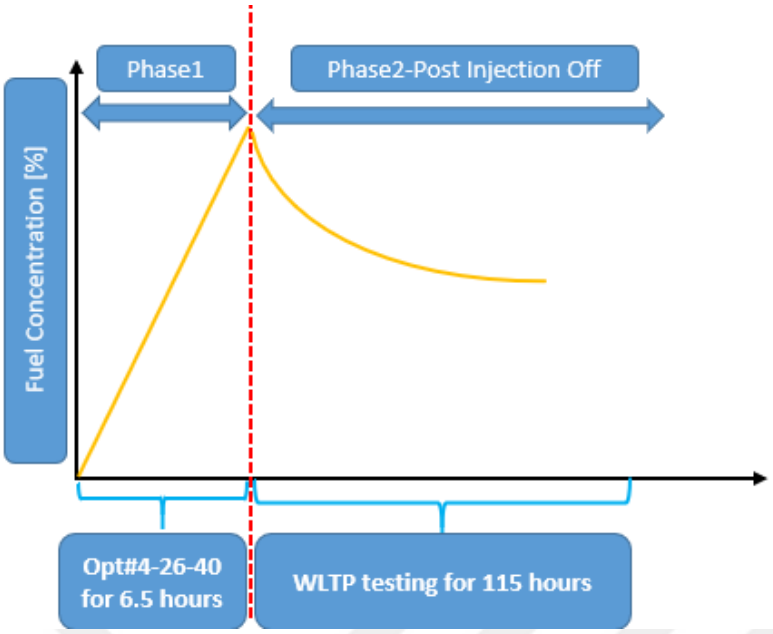

Figure 2.5 : Oil dilution recovery test plan.

2.4 Transient Tests

Vehicle speed histograms for five different cycle types are shown in Figure 2.6. The rate of oil dilution formation can vary between other driving profiles because these various vehicle speed profiles require particular speed and load conditions. Moreover, the second post quantity was changing between these cycles to hold DPF inlet temperature at 600°C. The controller was placed for the second post-injection quantity. Exhaust gas temperature at the inlet of DPF was kept at 600°C for these cycles by adjusting the second post-injection. 600°C target temperature was selected based on the active regeneration operating window. That means less second post-injection quantity demand for the cycles with a high engine out temperature due to high power demand. The purpose of transient testing was to investigate the accuracy of the modelling approach on steady-state test data over representative and challenging conditions.

Different drive cycles contain the various spray and wall interactions due to charge conditions in the cylinder, and changing the second post-injection quantity also increases the variety. In terms of position intolerance, two different engines were used during the transient tests to investigate the model results over different engines.

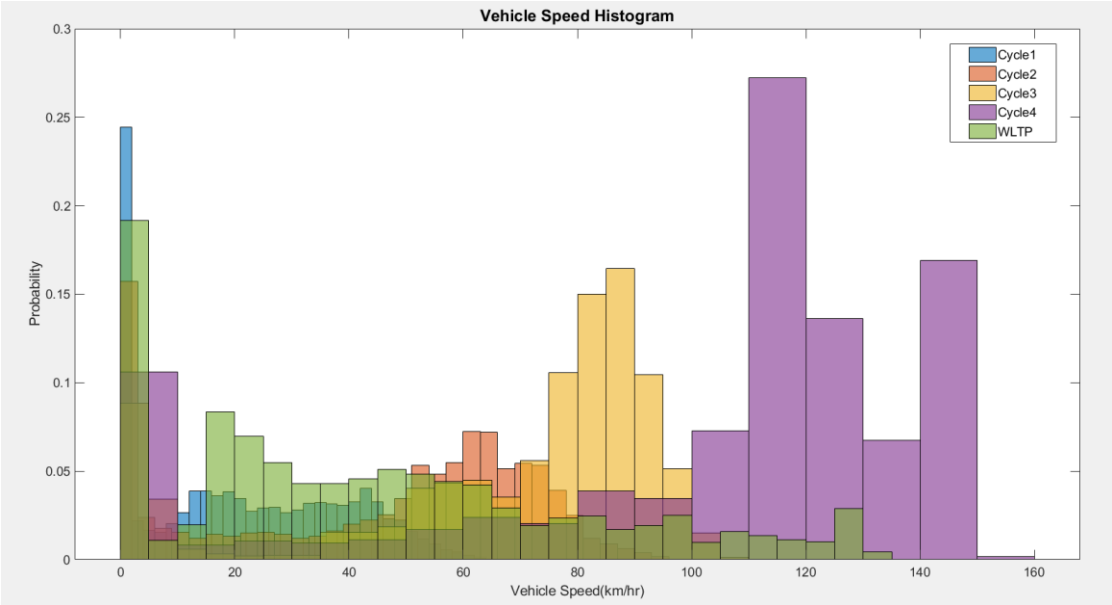

Figure 2.6 : Vehicle speed histogram.

2.5 Oil Dilution Measurement

Several different measurement techniques can be used to analyze fuel concentration in engine oil [4]. These measurement methods can be divided into three groups. The first measurement method evaluates the oil dilution rate by comparing total hydrocarbons at tailpipe by emission measurement devices and fuel flow measurements. Comparing total hydrocarbons at tailpipe by emission measurement devices and fuel flow measurements enables representative figures on oil dilution rate rather than absolute figures. In theory, this method can result in comparable figures. Yet, the combined error for fuel flow, airflow, and tailpipe emission measurements is way beyond these differences. Therefore, sustaining measurement consistency for the three sub-measurement systems required for this method in practice is not possible. The second measurement method evaluates the oil properties, such as kinematic viscosity, to understand its deviation from the initial sample. However, oil dilution due to fuel concentration is not the only parameter that might change the kinematic viscosity of the oil. So, a detailed assessment with this measurement technique is not possible. The third measurement method is Gas Chromatography & Flame Ionization Detector (GC&FID), which is the best practice among all three options in terms of accuracy. With GC&FID, fuel concentration in oil samples is directly measured rather than in-direct methods. Therefore, the accuracy of GC&FID does not get affected by the accuracy of multiple measuring elements or any other factor that influences the

physical oil properties. But this technique is an offline measurement and requires 4-6 hours in total for testing to reach a measurable range and measurement.

Figure 2.7 : Gas Chromatography & Flame Ionization Detector.

In total, 199 oil samples were analyzed during this study with GC&FID regarding ASTM3524 Standard Test Method for Diesel Fuel Diluent in Used Diesel Engine Oils by Gas Chromatography [14]. The GC device used for these analyses was AGILENT 6890N and equipped with AGILENT DB-1 Column type. A Flame Ionization Detector (FID) was paired with a gas chromatography instrument. FID uses the flame to ionize organic compounds containing carbon. Following separation of the sample in the GC column, each analyte passes through a flame, fueled by hydrogen and zero air, which ionizes the carbon atoms. Once formed, the ions are collected and measured to create a current at the detector's electrodes. The current is produced as the sensor collects the charged ions. The current is then converted to an electrical signal. [15]. The fuel mass fraction in the oil samples was measured with GC. GC results of diesel fuel, engine oil and pre-mixed samples are shown in Figure 2.8. A clear separation between oil and fuel in GC results was observed for lighter components below C20 and heavier components beyond C25. However, the molecules between C20 and C25 could not be measured directly since these fuel molecules were overlapped with the oil molecules. Therefore, the amount of C20 to C25 was estimated based on heavier measurable components. The ratio between C18-C19 and C20-C25 was calculated based on diesel fuel GC results. And, the ratio was applied to the results with the assumption of no evaporation between C18-C25. After the approach was validated with pre-mixed samples of 5-8% of the fuel mixture, test samples were measured.

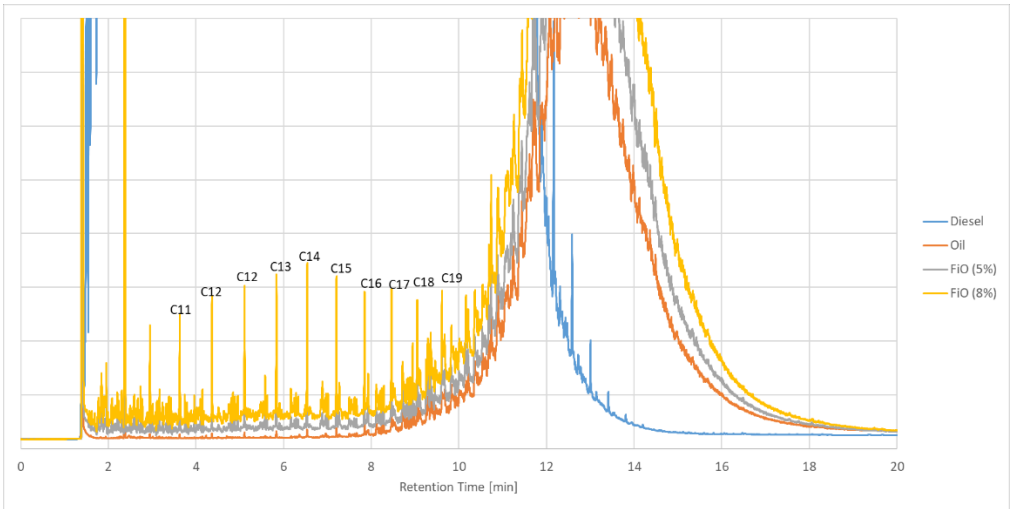

Figure 2.8 : Example of the chromatogram for diluted oil.

3. TESTING RESULTS

Results of fuel recovery testing are essential to calculate the gross oil dilution formation rate in the rest of the testing activities. Measurement results for collected oil samples during steady-state and transient tests contain the effect of fuel recovery. Thus, fuel recovery must be excluded to calculate the actual fuel rate going into the oil pan. Firstly, fuel recovery sample results were handled, and then the effect of fuel recovery was inverted in steady-state and transient oil sample results.

3.1 Recovery Test Result

The results of the oil recovery characterization test were shown in Figure 3.1. Fuel in oil concentration was measured as 14% by GC&FID at the beginning of the evaporation phase. There wasn't any injection after 30CA aTDC during the evaporation phase. Thus, additional oil dilution at that phase was not generated.

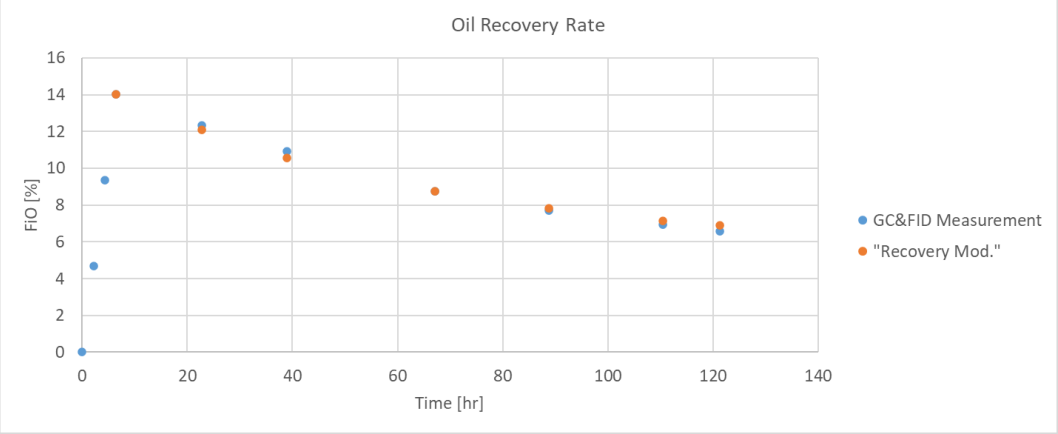

Figure 3.1 : Fuel recovery test results with the recovery model.

At the beginning of the evaporation phase, a significant drop in fuel in oil concentration was observed. However, the drop rate of the fuel in oil concentration over time reduced, and the oil dilution became almost constant after 100hr of WLTP testing without post injections. Similar behaviour was observed in Wattrus et al. [6] and Ito et al. [16]. Both light and heavy fractions were available at the beginning of the evaporation phase; therefore drop in oil dilution level was observed. However,

once the concentration of light fraction was reduced during the evaporation phase, the decrease rate of oil dilution was reduced and finally faded out. Thus, 40% of initial oil dilution could not be recovered at the end of the evaporation phase.

Fuel recovery testing aimed to cancel out the effect of recovery over steady-state and transient test results. Therefore gross formation rate of oil dilution could be calculated for each steady-state test point and transient test. In order to estimate the impact of oil recovery, asymptotic behaviour observed during testing needed to be reflected by a model. Exponential expressions can recall such an asymptotic behaviour as a function of testing duration. When heavy fraction (40% of initial oil dilution in this case) was subtracted from all evaporation phase results, and exponential curve fitting as a function of testing duration was applied, an equation with two components was obtained. The summation of these two components gave oil dilution at a specific time of evaporation testing. A simplified version of this equation was given in Eq (1). With that equation, each steady-state and transient test result were projected to gross oil dilution. The modelled value shown in Figure 3.1 was obtained based on Eq(1) with constants shown in Table 3.1. Modelled value was calculated for the evaporation phase of recovery characterization testing. First constant (C_1) represents portion of fuel cannot be recovered which is heavy fraction of fuel in oil. Second constant (C_2) indicates recovery rate of fuel in oil for light fuel fraction.

$$FiO_{final} = FiO_{init}(C_1 + (1 - C_1)e^{(-time*C_2)}) \quad (3.1)$$

Table 3.1 : Fuel recovery equation constants.

C_1	C_2
0.4	0.00000453

FiO_{init} term in Eq(1) was computed to calculate the gross oil dilution formation rate in the rest of the study.

3.2 Steady-State Test Results

GC&FID measurement results for steady-state test samples are shown in Figure 3.2. The testing duration between test points in the steady-state test matrix was deviating to have more efficient testing. Comparing the different steady-state test points with

each other is only possible after these results are processed. In each steady-state test point, a second sample was collected at the middle of the testing duration. Therefore, having the almost identical yellow and blue bars length indicated that steady-state test results did not show any outliers.

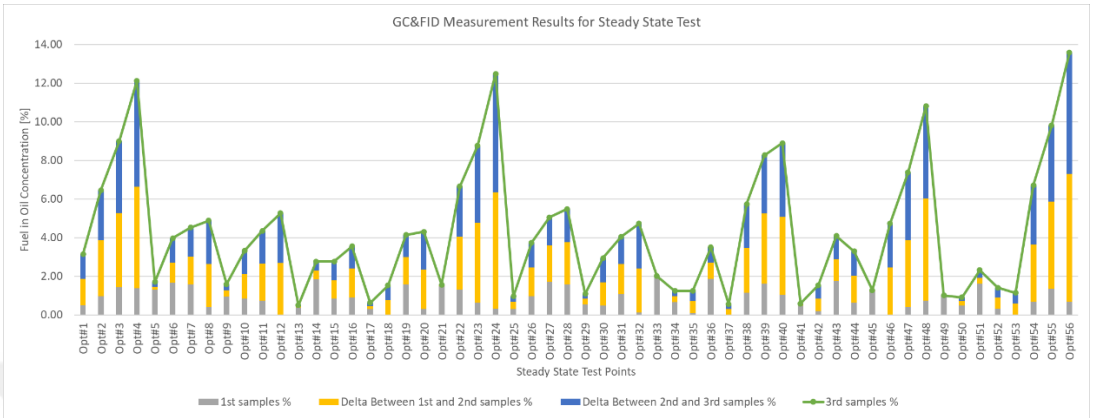

Figure 3.2 : Steady-state test results.

As discussed earlier, oil dilution results from the balance between fuel addition to the oil pan and fuel removal from the oil pan. During the steady-state tests, fuel concentration measurements were showing a difference between fuel addition and removal. For further studies, steady-state measurements were corrected to fuel addition to oil, called gross oil dilution formation rate. The equation obtained based on recovery data was used to calculate gross oil dilution from net oil dilution by calculating FiO_{init} for each test point in the steady-state test matrix. Effect of oil recovery correction shown in Figure 3.3 for Opt#1. In Figure 3.3, corrected fuel concentration was given together with actual fuel concentration measurement. Although fuel recovery was expected to be minimal on test results because fuel recovery requires a longer duration to be effective, the correction was applied to include fuel recovery in the results. Oil dilution recovery characterization over WLTP was directly used to calculate gross oil dilution rate in all steady-state test points. The effect of oil dilution recovery upon steady-state test results was minimal.

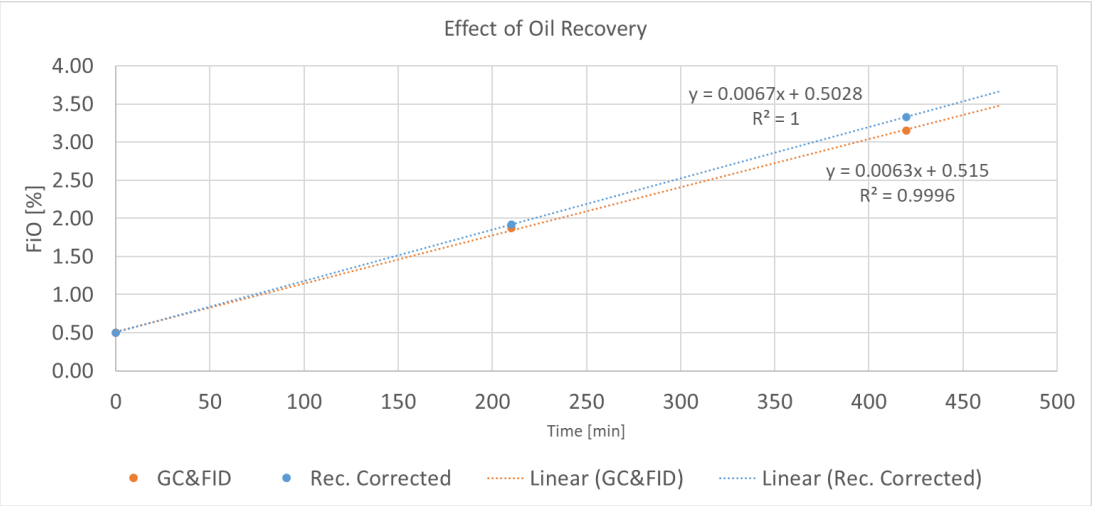

Figure 3.3 : Recovery correction to calculate gross fuel addition in Opt#1.

The slope of the linear curve fit to corrected fuel concentration in each test point gives the rate of gross fuel addition to oil pan with information of oil volume was 3.8 Liter in all test points. The gross oil dilution formation rate is given in Figure 3.4. The steady-state test matrix pattern allowed the calculation of the gross oil dilution rate for each post-injection separately. Blue bars in Figure 3.4 represent the gross oil dilution rate due to the first post-injection in each group over the rest of the test points in the same group.

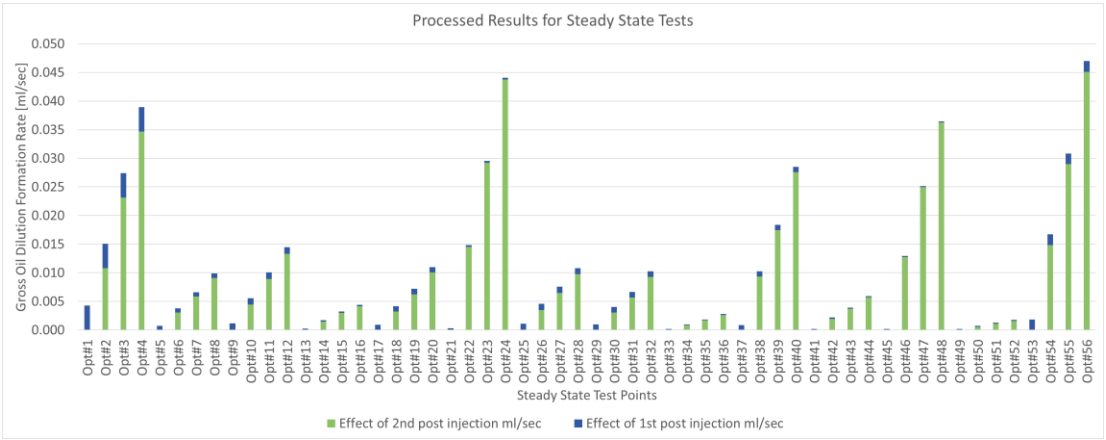

Figure 3.4 : Gross oil dilution formation rate for steady-state test points.

Injection timing for the first post-injection was within the range of 30 – 50 CA aTDC, where timing for the second post-injection was set in 120 – 150 CA aTDC. Thus, in parallel to the literature review, the effect of first post-injection upon oil dilution stayed limited compared to the second post-injection, which was injected into the relatively less dense ambient resulting in higher oil dilution impact.

3.3 Transient Test Results

Recovery corrected oil dilution results for the transient tests are shown in Figure 3.5. Cycle#1 had the lowest vehicle speed distribution among all other cycles, and Cycle#4 had the highest average vehicle speed. When Cycle#4 and Cycle#1 compared, the influence of vehicle speed profile over oil dilution formation rate can be seen. During transient tests, DPF inlet temperature was kept constant at 600°C over the cycles by controlling the second post-injection quantity. The necessity of a second post-injection was low in high vehicle speed cycles due to higher engine out temperature. In addition to that, post injections were sprayed into denser ambient in high load conditions. Therefore, high vehicle speed cycles like Cycle#4 resulted in less oil dilution than Cycle#1.

The first four measurements shown in Figure 3.5 belong to the first engine tested, and the rest belong to the second engine tested during transient tests.

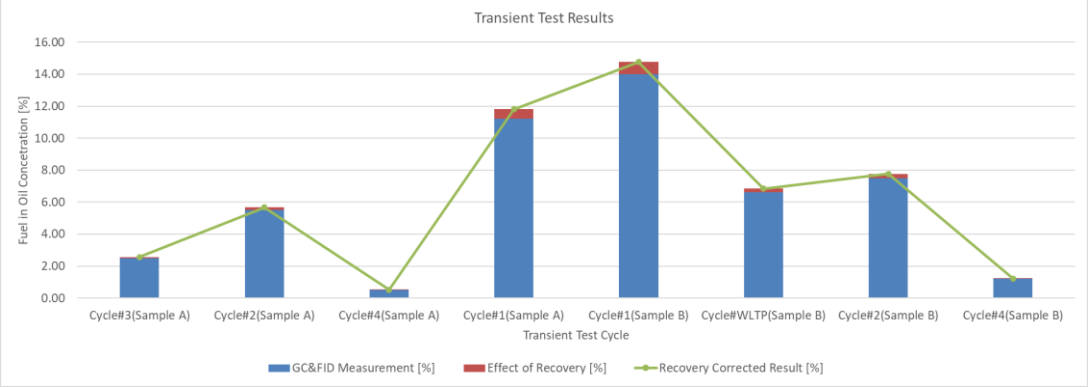

Figure 3.5 : Transient test results.

4. MODELLING

4.1 Input Parameter Calculation

Studies regarding the correlation between SMD and oil dilution formation rate during the literature investigation phase were seen. In addition to SMD, spray penetration depth was also mentioned as one of the critical parameters for correlation between spray parameters and oil dilution formation rate. The primary mechanism for oil dilution is unburnt fuel hitting the cylinder walls. If the unburnt fuel does not reach the cylinder walls, the oil dilution formation rate will be minimal. There are several methods for the calculation of spray parameters in the literature. For the estimation of spray parameters, Hiroyasu and Arai's equations will be used as shown below.[17]

$$x_{32} = 2.33 * 10^{-3} * \Delta P^{-0.135} * {\rho_{air}}^{0.121} * Q^{0.131} \tag{4.1}$$

$$t_b = 28.65 * \rho_{liq} * D * \left(\rho_{liq} * \Delta P\right)^{-0.5} \tag{4.2}$$

$$0 < t < t_b \rightarrow S = 0.39 * (2 * \Delta P/\rho_{air})^{0.5} * t \tag{4.3}$$

$$t > t_b \rightarrow S = 2.95 * (\Delta P/\rho_{air})^{0.25} * (D * t)^{0.5} \tag{4.4}$$

When Hiroyasu and Arai's equations were introduced, validation of these equations within the working boundaries of today's systems was not completed. With further studies on these equations, verification of the equations within the operating range that these study covers were constructed by Xinyi et al. [18].

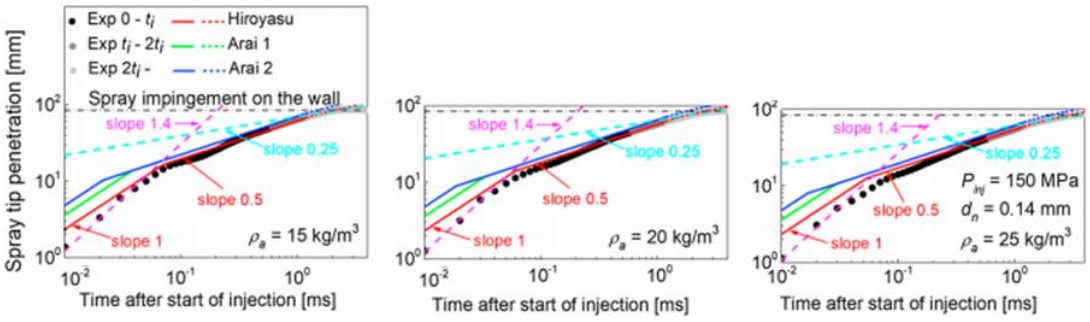

Figure 4.1 : Validation of spray parameters for wider operational range [18].

In Figure 4.1, Hiroyasu and Arai's equation validation for the range of 150MPa injection pressure was shown in Xinyi et al. studies. The maximum rail pressure tested for this study is 105MPa. In Figure 4.1, black and grey dots show experimental results for spray penetration depth, and colouring goes to grey from black when injection duration is increased. The red curve represents Hiroyasu's equation which shows good alignment with experimental results.

When the parameters are checked in SMD and spray penetration equations, several parameters require further calculations, such as in-cylinder air density in injection timing. A sub-calculation to determine cylinder volume in injection timing based on Figure 4.2 was done for that purpose. Air mass flow was measured with a build-in flow measurement sensor which works with hot film methodology. Air mass flow was converted to air mass in each cylinder, with engine speed information measured with the hall speed sensor.

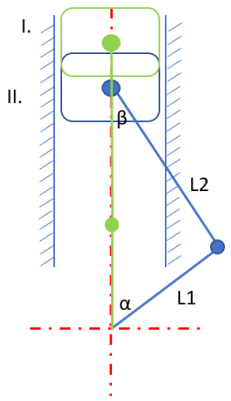

For Location #I,

$$\frac{\frac{Engine\ Vol.}{Number\ of\ Cyl.}}{\frac{Cylinder\ Dia^2 * \pi}{4}} = 2 * L1$$

$$\frac{2 * L1}{Comp.Ratio - 1} * \frac{Cylinder\ Dia^2 * \pi}{4} = Dead\ volume$$

For any Location #II,

$$Volume = (L1 + L2 - L1 * cos\alpha - L2 * cos\beta) * \frac{Cylinder\ Dia^2 * \pi}{4} + Dead\ volume$$

$$\beta = \text{asin}(\frac{L1}{L2} * \sin\alpha)$$

For air density calculation,

$$Air\ density = \frac{Air\ flow}{Volume}$$

Figure 4.2 : Calculation of air density.

The density of the fuel is taken as a constant. In-cylinder pressure was measured during steady-state tests, so this parameter is directly taken from measurements with AVL GH14P glow-plug pressure sensors. Injectors with 8 holes and 0.108mm hole diameter are used during testing. L/D ratio for the injectors was 6.3. Penetration depth is normalized based on the distance from the injector nozzle to the cylinder wall. The length used for the normalization of spray penetration depth is shown in Figure 4.3.

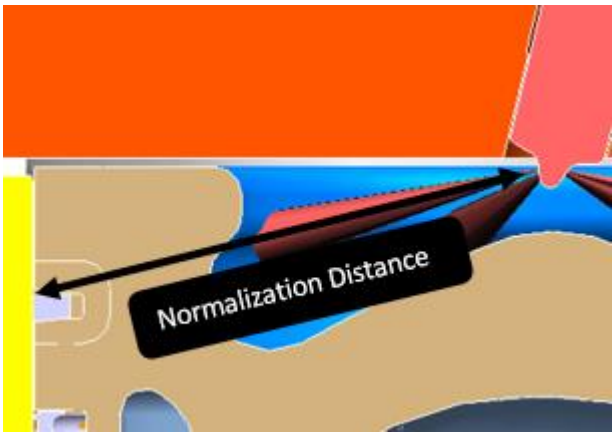

Figure 4.3 : Normalization distance.

As a result of normalization, 1 means that fuel spray is hitting the cylinder wall, and any number below 1 means that fuel spray is not reaching the cylinder wall.

Equations also contain injector nozzle opening duration. External fuel flow measurement was placed based on the Coriolis effect to define the correlation between injector valve opening duration and quantity demand. Surface regression was obtained based on fuel flow measurement at different valve opening durations and rail pressures. This surface is shown in Figure 4.4 after being scaled based on minimum and maximum actual measured values.

		Rail Pressure [MPa]											
		10	20	25	30	40	50	60	70	80	90	100	120
Injection Volumetric Demand [mm^3/mm^3]	0.04	9	5	3	2	2	1	1	1	0	0	0	-
	0.91	10	7	5	4	3	2	2	2	2	1	1	1
	1.82	12	9	8	6	4	4	3	3	3	2	2	2
	2.27	12	10	8	7	5	4	3	3	3	3	3	3
	2.73	13	11	9	7	5	4	4	4	3	3	3	3
	3.18	14	11	10	8	6	5	4	4	4	3	3	3
	3.64	15	12	11	9	7	5	4	4	4	4	3	3
	5.45	18	14	13	11	8	7	6	5	4	4	4	4
	7.27	21	16	14	12	10	8	7	6	5	5	4	4
	10.91	26	20	17	15	11	10	9	8	7	6	6	5
	16.36	33	26	22	19	15	12	10	10	8	8	7	6
	23.64	42	32	27	23	18	15	13	12	11	10	9	8
	32.73	52	40	34	29	23	19	16	15	13	12	11	10
	43.64	63	49	43	36	28	23	20	18	16	15	14	12
	60.00	74	60	53	47	36	29	25	22	20	19	18	15
	76.36	87	73	65	56	45	37	32	28	26	24	22	20
	100.00	100	85	78	71	58	48	41	36	32	30	28	25

Figure 4.4 : Fuel injector scaled characterization data.

Matlab environment was used to do the calculations. Calculation of air density at the post-injection timing was reflected in Matlab Simulink, as shown in Figure 4.5. The same expression shown in Figure 4.2 was applied for the calculation of air density in Matlab. Since the study has lots of data from both steady-state and transient tests, the combination of Matlab and Python environment helped create a semi-automated pipeline for calculating the results.

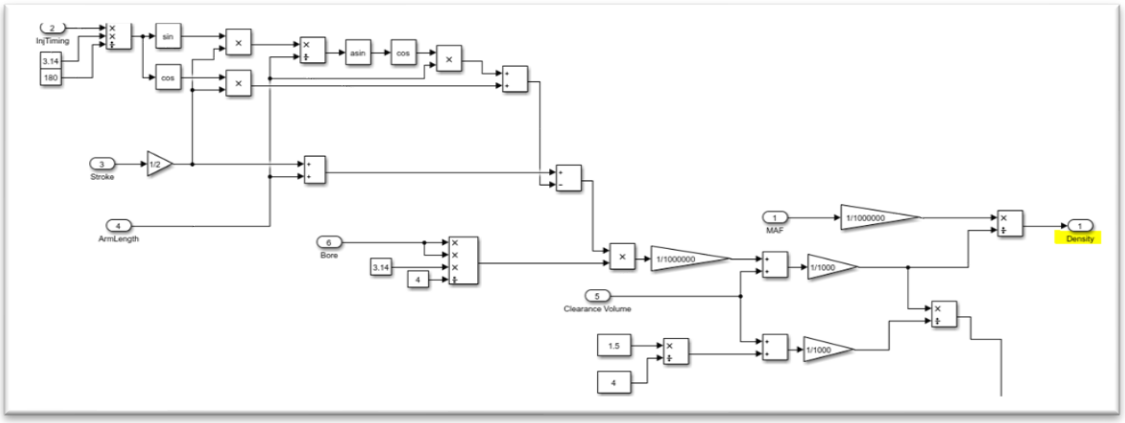

Figure 4.5 : Calculation of air density in Matlab.

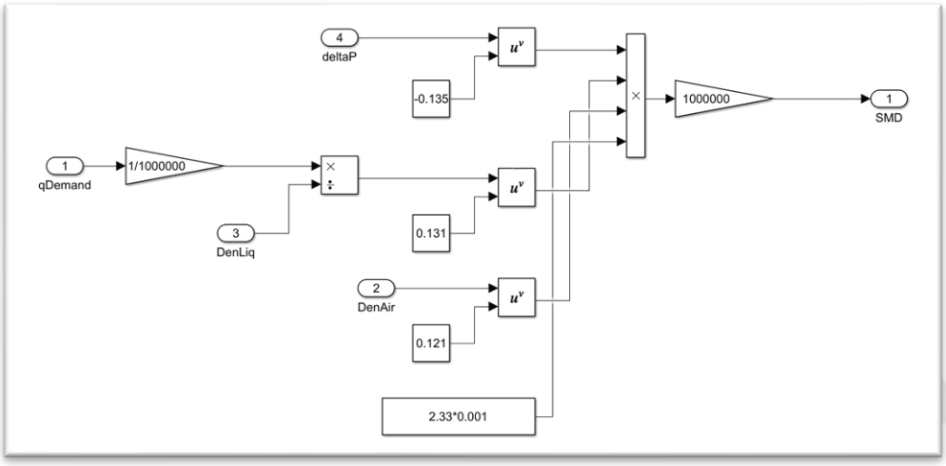

Figure 4.6 : Calculation of SMD in Matlab.

The equation shown in Eq(2) is reflected in the Matlab Simulink environment. Detail of the SMD calculation in Matlab is shown in Figure 4.6.

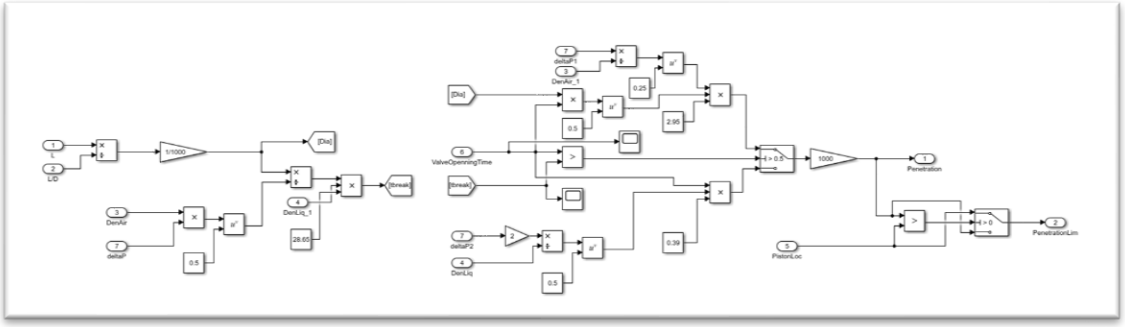

Figure 4.7: Calculation of penetration depth calculation in Matlab.

In Figure 4.7, details of normalized spray penetration depth are shared regarding the equation given in Eq(3), Eq(4) and Eq(5). The Break-up timing limit is calculated on

the left side. The correct penetration equation is selected from the switch based on the break-up timing limit parallel to Hirayu and Aria's definitions.

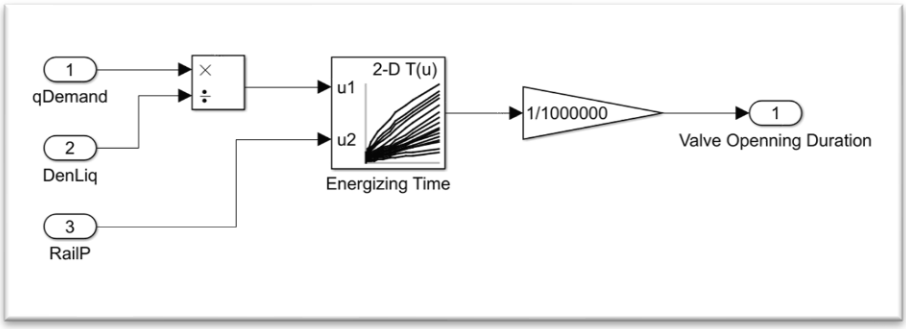

Figure 4.8 : Calculation of valve opening duration in Matlab.

Valve opening duration characterization surface is also implemented in Matlab environment with a 2D Look-Up table as shown in Figure 4.8. Unit transformation to second from microsecond is applied for further use of this parameter.

Another critical parameter for SMD and penetration depth calculation was delta pressure between rail pressure and in-cylinder gas pressure in post-injection timing. Delta pressure is introduced with "DeltaP" naming in model structure in Figure 4.6 and Figure 4.7. In-cylinder pressure was measured at specific crank angles during steady-state tests. Therefore, a method to arbitrate in-cylinder pressure at post-injection timing was required. Polynomial fit applied to anchor points of in-cylinder pressure models at different crank angles. When in-cylinder pressure is needed at a specific crank angle, the polynomial fit is solved at that particular point and fed into delta pressure calculation for the spray parameter.

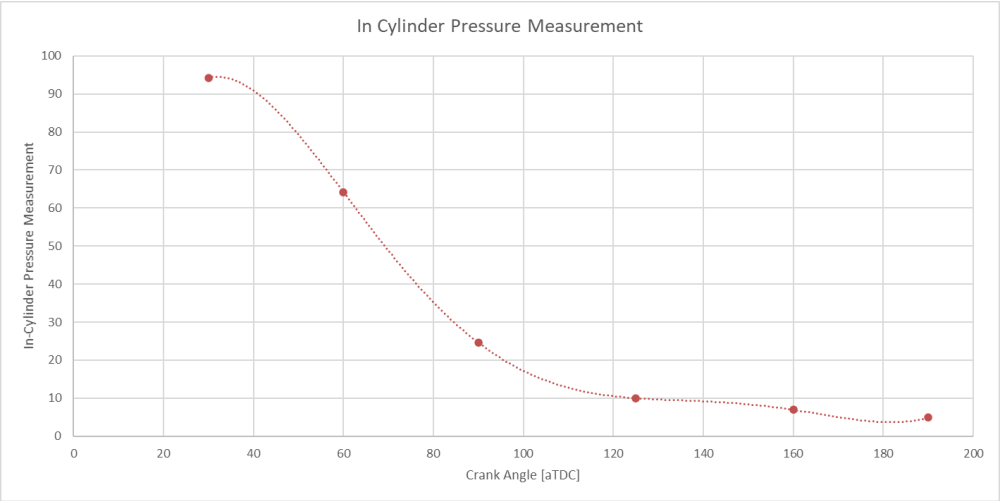

Figure 4.9 : Example of polynomial fitting to in-cylinder pressure measurement.

Code to execute in-cylinder pressure at a required crank angle is shown in Figure 4.10.

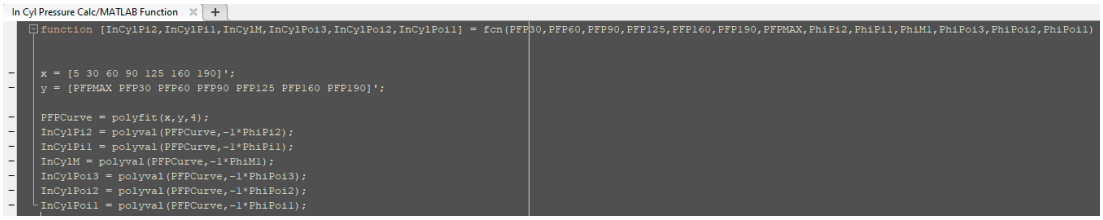

Figure 4.10 : Embedded code running in Matlab Simulink.

In Figure 4.11, post-injection quantity is swept starting from 1mg/stroke up to 10 mg/stroke for 1500RPM – 5bar load test point (Opt#10-11-12). There is an increase in both SMD and normalized penetration depth with an increase in post-injection quantity demand. With the increase of flow demand, SMD equations show an increase with the 0.131 power of increase in flow demand. And also, normalized spray penetration shows an increase with the power of 0.5 of increasing fuelling duration to achieve demanded increasing post-injection quantity.

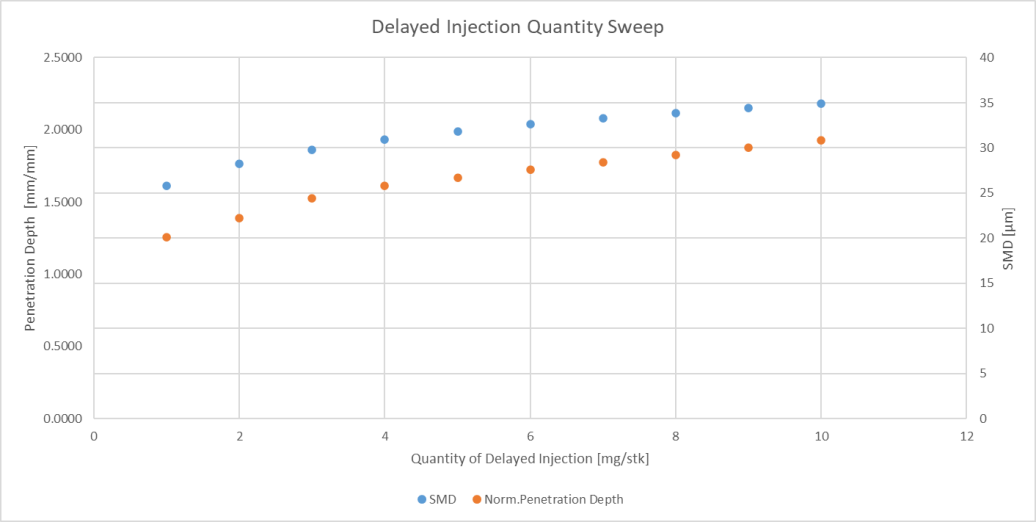

Figure 4.11 : Post-injection quantity swept.

In Figure 4.12, the timing for post-injection is swept starting from 70CA aTDC up to 170CA aTDC for 1500RPM – 5bar load test point (Opt#10-11-12). When the injection timing for post-injection goes towards TDC, in-cylinder pressure is increased together with in-cylinder gas density at the timing of post-injection. As a result of the air density increase, SMD is increased with the power of 0.121 of air density increase. And also, SMD is increased very minorly due to lowered delta between rail pressure and in-cylinder pressure due to delta pressure term in the SMD equation. Compared to the

magnitude of rail pressure and in-cylinder pressure, it can be noticed that the effect of in-cylinder pressure change on delta pressure term is quite limited. Normalized penetration depth is lowered with the power of 0.25 of increased air density for the equation valid after break-up timing. Similar to SMD, delta pressure between rail pressure and in-cylinder pressure at the timing of post-injection influences normalized spray penetration depth calculation. Again, the effect of in-cylinder pressure change on delta pressure term stayed minimal compared to rail pressure.

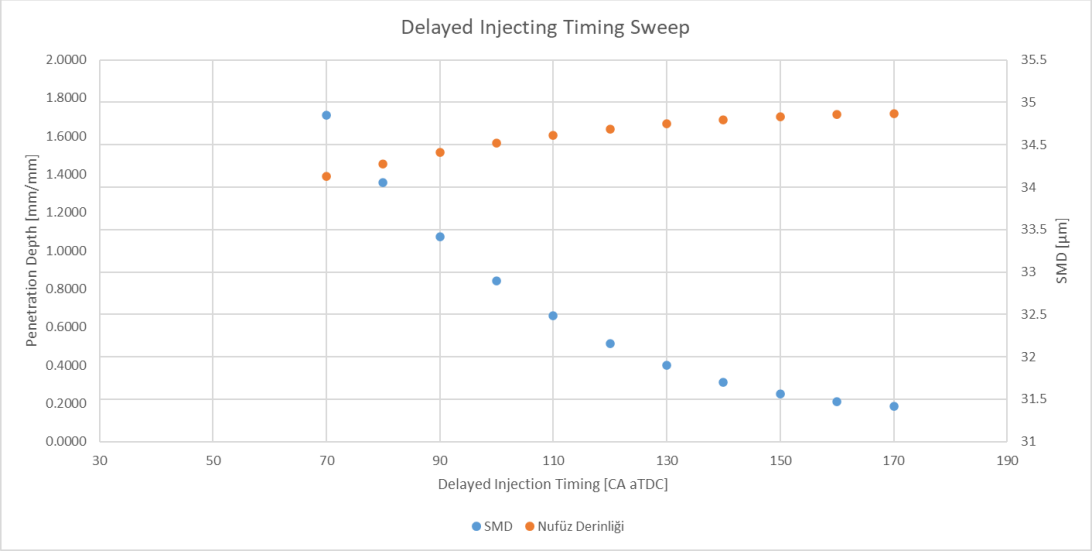

Figure 4.12 : Post-injection timing swept.

In Figure 4.13, rail pressure sweeps are given. There are several effects of changing rail pressure. With increasing rail pressure, delta pressure between rail pressure and in-cylinder gas pressure rise directly. SMD equation response to that increase with the power of 0.131 of the increase in delta pressure. As a result of delta pressure increase, SMD is decreased responding to rail pressure increase. In terms of normalized spray penetration depth, two terms are directly affected by rail pressure change. With increasing rail pressure, delta pressure increased instantly, and injector valve opening duration is reduced due to increased delta pressure. Under the influence of these two terms, the normalized spray penetration depth is first raised with increasing rail pressure. It drops when rail pressure is further increased due to reduced injector valve opening duration for the same amount of post-injection quantity.

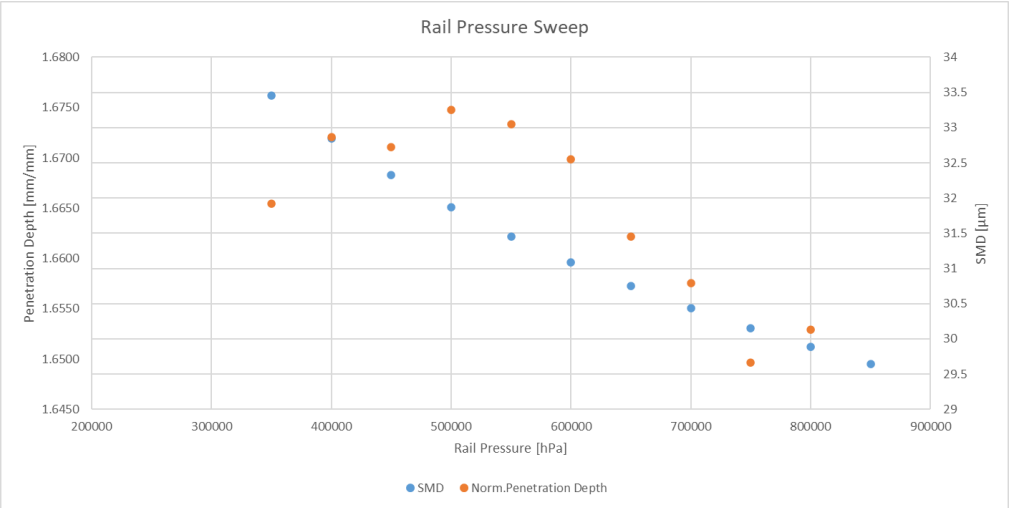

Figure 4.13 : Rail pressure swept.

Based on the isentropic compression equation, the temperature at the needed crank angle is calculated as shown in Figure 4.14. Temperature measurement at exhaust manifold is assigned to temperature at Point#4. Similar to other parameters, calculation of in-cylinder temperature estimation was done in Matlab Simulink and included in the pipeline.

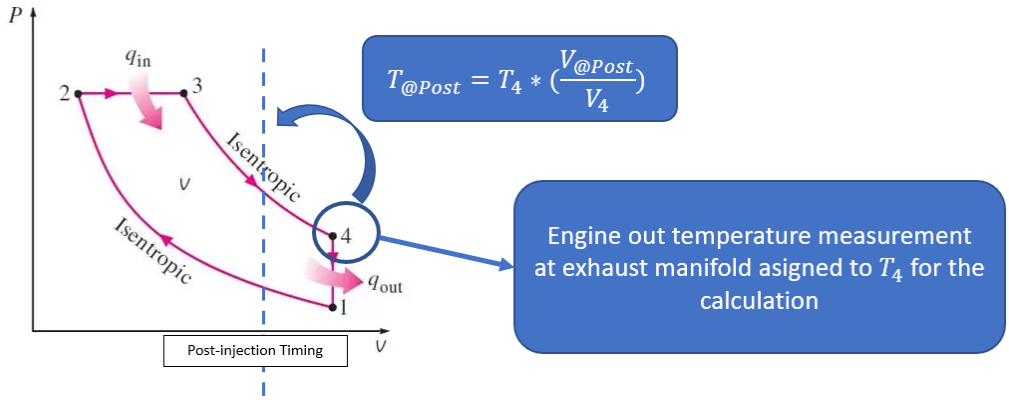

Figure 4.14 : Calculation of in-cylinder temperature.

4.2 Correlation Investigation

The df.corr() command from Python Pandas library was used to investigate the correlation between several input parameters and oil dilution rate. Figure 4.16 was obtained as output from the Python code shown in Figure 4.15.

```
import warnings
warnings.filterwarnings("ignore")
import pandas as pd

data = pd.read_excel('Data_OilDil.xlsx')

print(data.describe(include = 'all'))
print(data.dtypes)
data_cor = data.corr(method = 'pearson')
data_cor = data_cor.round(decimals=3)
print(data_cor)
```

Figure 4.15 : Correlation matrix code.

In Figure 4.16, the correlation matrix for oil dilution formation rate was shown based on Pearson coefficients. The strongest correlation was observed with normalized penetration depth. Delta between previous injection, in-cylinder pressure and temperature at post-injection timing showed a strong correlation with oil dilution formation rate.

Param	*Eng.Spd*	*Oil Dil.Rate*	*In-Cyl. Pres*	*SMD*	*Norm.Penet.*	*In-Cyl. Temp*	*phMain*	*DeltawithPrev*
Eng.Spd	1	0.203	-0.031	-0.191	-0.026	0.009	0.712	0.155
Oil Dil.Rate	0.203	1	-0.409	-0.204	0.733	-0.385	0.062	0.495
In-Cyl. Pres	-0.031	-0.409	1	0.701	-0.815	0.935	0.038	-0.924
SMD	-0.191	-0.204	0.701	1	-0.415	0.781	-0.169	-0.804
Norm.Penet.	-0.026	0.733	-0.815	-0.415	1	-0.772	-0.185	0.807
In-Cyl. Temp	0.009	-0.385	0.935	0.781	-0.772	1	-0.021	-0.974
phMain	0.712	0.062	0.038	-0.169	-0.185	-0.021	1	0.112
DeltawithPrev	0.155	0.495	-0.924	-0.804	0.807	-0.974	0.112	1

Figure 4.16 : Correlation between oil dilution formation rate and several parameters.

However, some of the parameters were direct or indirect input to the normalized penetration depth calculation. Therefore, the delta between previous injection, in-cylinder pressure, and temperature showed a good correlation with normalized penetration depth. Thus, these parameters were not expected to contribute to the correlation any further in modelling studies. Yet, the start of injection timing delta with the previous injection was also evaluated as an input in the study to see this expected behaviour. Oil dilution formation rate and engine speed showed a certain level of correlation. However, the correlation between normalized penetration depth and engine speed was minimal. Therefore engine speed was evaluated as an input. Engine speed determines the frequency of post injections which will occur within a certain period. When oil dilution formation rate is considered, engine speed determines how many times the incident causing oil dilution happens for a specific period.

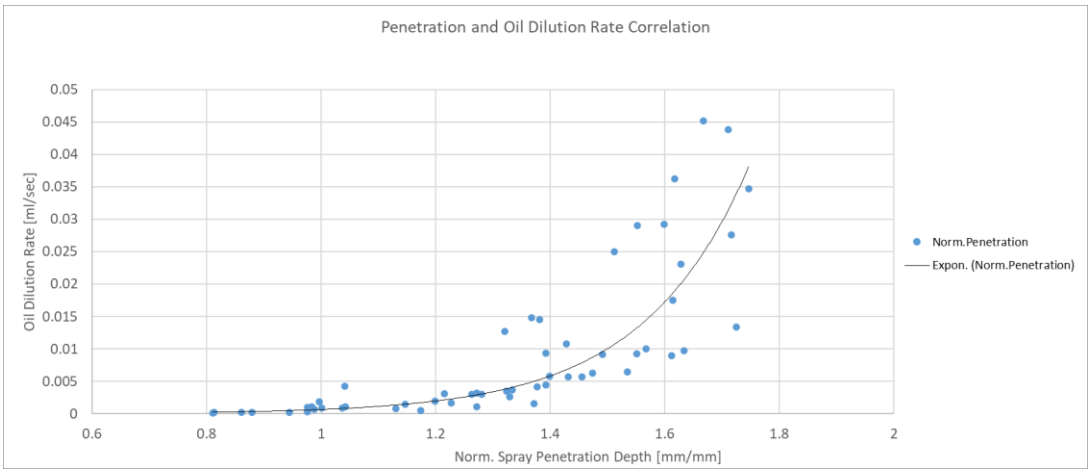

Figure 4.17 : Correlation between normalized penetration and oil dilution rate.

Spray penetration depth was normalized based on distance from injector nozzle to the cylinder wall, so 1 means that the spray reached up to cylinder wall in Figure 4.17. As shown in Figure 4.17, there is a specific correlation between normalized penetration depth and gross oil dilution formation rate. The possibility of oil dilution formation was minimal when normalized penetration below 1 since normalized penetration depth below 1 indicates minimal fuel spray and cylinder wall interaction. The piston location might have been influenced if the test matrix included test points with post-injection timing before 30 CA aTDC.

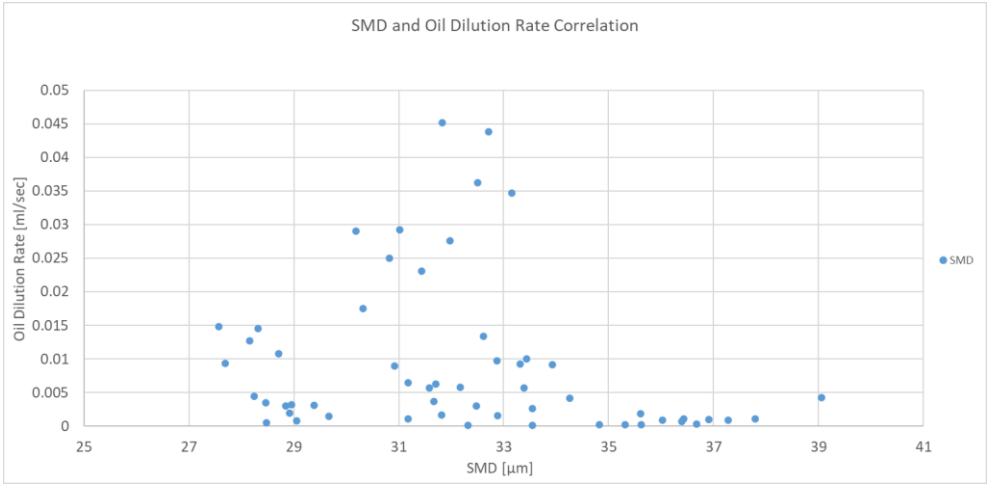

Figure 4.18 : SMD and oil dilution rate correlation.

If SMD were increased by increasing post-injection quantity, penetration would be increased in line with SMD increase. Therefore, the oil dilution rate as a result of the increasing post-injection amount will be increased. Therefore, a correlation between oil dilution rate and SMD can be mentioned in such a case. But if post-injection timing

were advanced, SMD would be increased, yet spray penetration would be decreased. In such a case, the oil dilution rate was expected to be reduced based on the literature review. As the test matrix includes different post-injection timings and quantities, a direct correlation between SMD and oil dilution rate was not observed in Figure 4.18. However, the correlation between SMD and oil dilution rate can be seen in Figure 4.19 when test points were filtered based on normalized penetration depth within 1.13-1.22mm/mm range.

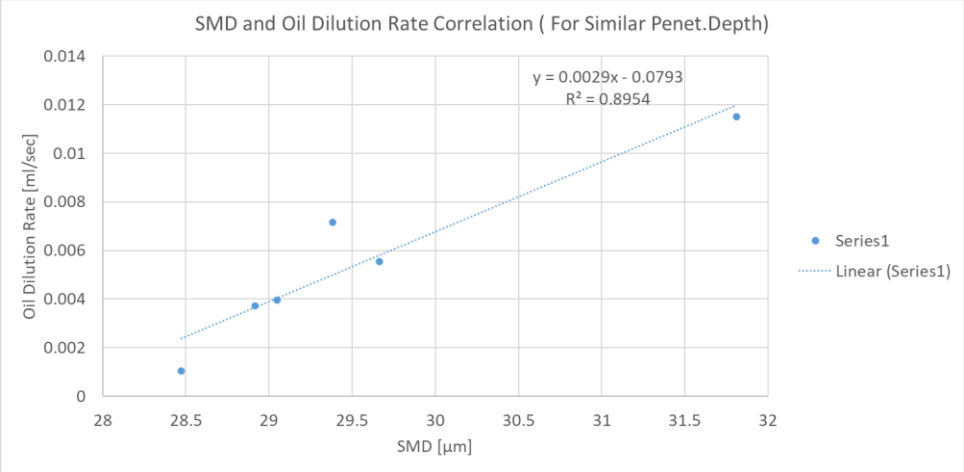

Figure 4.19 : SMD and oil dilution rate correlation in filtered data.

By now, the correlation between empirical spray parameters and gross oil dilution was indicated. To propose a modelling approach, the correlation observed with normalized penetration depth and SMD was combined. One of the additional parameters considered in this study was engine speed. The engine speed was also considered one of the input parameters to the modelling approach as the engine speed determines the frequency of post injections. The rate of oil dilution measured by GC&FID was a result of multiple post-injection within a certain period. Therefore, projecting the oil dilution rate to a reference engine speed was needed to keep the number of instances that caused oil dilution at the same level. When the same load condition pairs were compared, high engine speed resulted in a higher oil dilution rate, as shown in Figure 4.20.

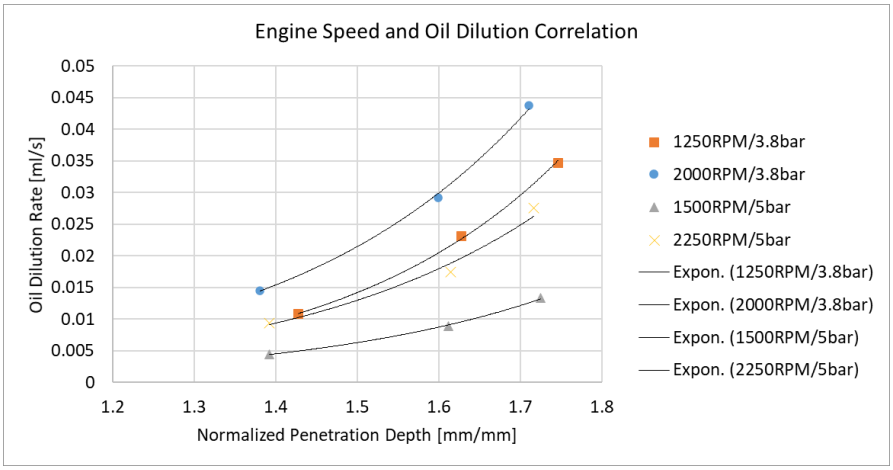

Figure 4.20 : Engine speed and oil dilution relation.

In conclusion, normalized penetration, Sauter mean diameter and engine speed were evaluated as the input set for the modelling activities. Based on the literature review, the coolant temperature was shown as an effective oil dilution parameter. However, the coolant temperature was kept at 90°C for all testing activities in this study. Therefore, the coolant temperature was not included in the models. In addition to these parameters, the timing delta between the previous injection was also investigated as an addition.

4.3 Polynomial Model

For calculation of the test and train accuracy, gridsearch from Python library was used as shown in Figure 4.21. That library function separates the input data into n sub-groups. The function uses $(n-1)$ sub-groups for model training and the remaining sub-group for calculation of test accuracy. For the calculation, 4 separate data groups were created as can be seen in the code. The gridsearch command did the fitting 4 times with 75% of the input data in every round and calculated average test and train accuracy.

```
53  parameters = {'fit_intercept':[False], 'normalize':[True], 'copy_X':[True, False]}
54  Grid_LR = GridSearchCV(lr,parameters,cv=4)
55  Grid_LR.fit(pf_degree.fit_transform(inputs),output)
56  Grid_LR.best_estimator_
57  scores_LR=Grid_LR.cv_results_
58  #print('Results for Poly2 Model',scores_LR['mean_test_score'])
59  print('------- Results for Poly2 Model-------')
60
61  for param,mean_val,mean_test in zip(scores_LR['params'],scores_LR['mean_test_score'],scores_LR['mean_train_score']):
62      print(param,'R^2 on test data:',mean_val,'R^2 on train data',mean_test,'total',mean_val+mean_test)
```

Figure 4.21 : Python code to execute gridsearch.

In order to show the success of the other modelling approaches on the prediction of oil dilution formation rate, polynomial regression was used as a reference. Two different input sets were tried out during polynomial regression studies. In Figure 4.22, results for the accuracy of both input sets in different polynomial degrees are shown. Bars in Figure 4.22 indicates the average accuracy of the polynomial regression over train data, and scatter plots with lines indicate average accuracy for test data. With the increasing number of degrees in polynomial regression, accuracy for train data increases. However, accuracy for test data starts to drop for both of the input sets. Any R^2 below zero is shown as zero to make the figure more readable. Although the second input set had better accuracy in train data, overfitting tendency increased with the second input set, and accuracy for test data was low compared to the first input set. As a result, second-degree polynomial fit with inputs of normalized penetration depth, SMD and engine speed was evaluated over transient test data to compare with Gaussian process regression results.

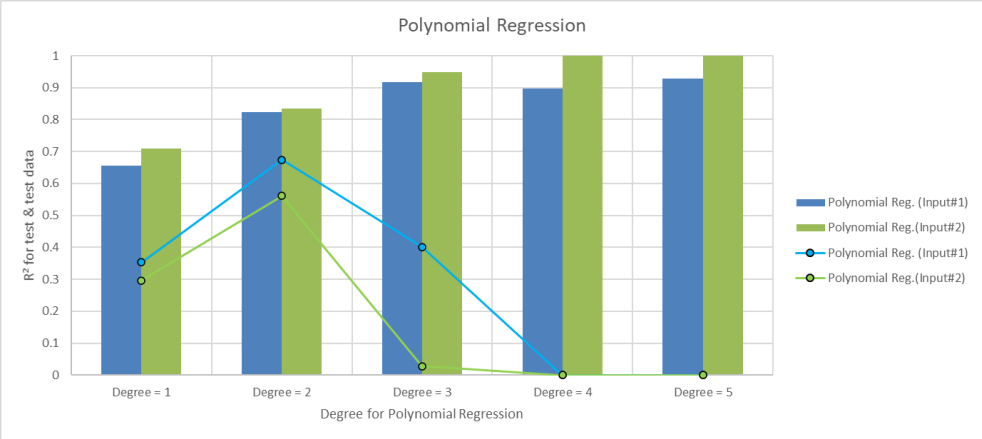

Figure 4.22 : Polynomial regression results.

4.4 Gaussian Process

As the formation rate of oil dilution was expected to be affected by several parameters, the modelling approach must be suitable for high dimensional problems. As time on the test bed and measuring samples were very expensive and time-consuming, the number of the measurements should be optimized and kept minimum as possible. Therefore, the modelling approach should build a good correlation with as few measurements as possible. Additional to these requirements, the modelling approach should be flexible enough so that that non-linear engine behaviours can also be

captured. Yet, model flexibility must never be too big to overcome overfitting risk. The modelling approach should give good figures of the train data hull. The computational load for modelling the formation rate of oil dilution is not a high importance requirement; as a matter of fact, the increasing number of measurements leads to a huge increase in testing duration and cost. For literature investigation, Gaussian process met these requirements [19], [20], [21].

Several different modelling approaches are used in engine models, such as polynomial regression, tree-based models, and machine learning algorithms. Each of these modelling approaches has its advantages and drawbacks.

Polynomial regression has several advantages compared to the Gaussian process. Polynomial models have a simple form, easy to understand and are well known. Furthermore, polynomial regression is computationally cheap and easy to implement engine controller units. Avoiding overfit by using statistical tests and removing parameters that are not significant is possible with polynomial regression. However, the main disadvantage of polynomial regression is the wrong extrapolation of the data. Polynomial models are tended very fast to high (positive or negative) values outside the region of the measurement data, where the Gaussian process do not. Moreover, low-order polynomials are not flexible enough to approximate any non-linear engine behaviour, and high-order polynomials tend to waviness.

Tree-based models divide the input space into smaller sub-spaces and assign a separate model for each subspace. And, the intersection between the individual models is smoothed to achieve a continuous model over the whole input space. Generally, if the engine mapping cannot be approximated by polynomials and the type of intersections do not suit the nature of the problem, then the number of sub-models and therefore the number of measurements will grow rapidly with tree-based modelling. With the Gaussian process, there is only one global model, and no sub-models exist.

The Gaussian process is one of the machine learning approaches, which also include support vector regression. Gaussian processes are kernel machines, whereas the support vector machine is sparse kernel machines. The Gaussian process can be computationally expensive. On the other hand, sparse kernel machines take a subset of measurements for prediction. Therefore, the predictions will not be as accurate as of the Gaussian process, but the support vector regression is computationally cheaper

than the Gaussian process. In the formation of oil dilution problem, computational load is not very important, but the accuracy of the modelling approach is critical.

As a result of these advantages and drawbacks, Gaussian process regression was selected to predict the formation rate of oil dilution.

$$k(x, x') = \exp\left(-\|x - x'\|^2 / 2l^2\right) \tag{4.5}$$

In Eq(6), the kernel function, which is called squared-exponential (SE), is shown. l is the length scale of the kernel.

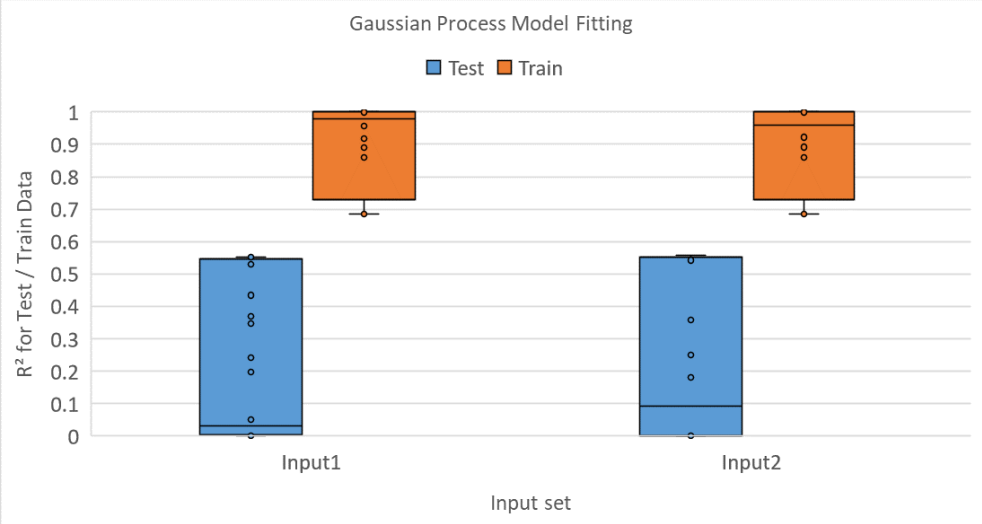

Figure 4.23 : Evaluation of two different input sets.

The Gaussian process is flexible enough to approximate non-linear engine behaviour. However, this brings over-fitting risks as well. To avoid overfitting during modelling, test data was segmented into four groups. Four iterations of model creation were done where three segments of the measurement data were used as train data, and the last segment was used as test data in each iteration similar to Polynomial model accuracy calculation. Average train and test accuracy results after positive saturation are shown in Figure 4.23 separately for two different input sets. Overfitting tendency was captured with average test accuracy.

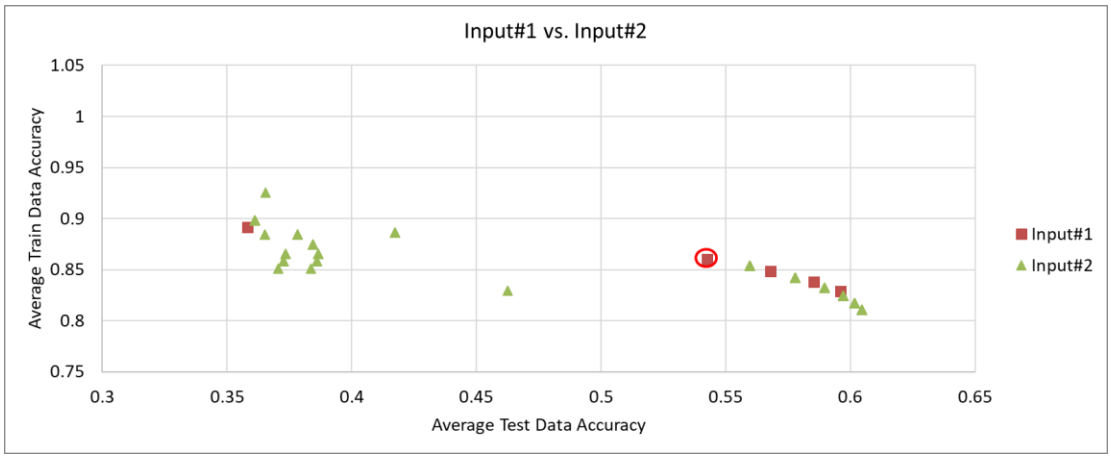

Figure 4.24 : Comparison of input sets for the Gaussian process.

When the input sets were compared in details by sweeping length scale, improvement in trade-off curve was not observed. Therefore, input#1 was determined as sufficient enough to have a good fitting. The selected model configuration also marked on Figure 4.24.

4.5 Cumulative Model Results

Transient data was recorded with separate files during testing. After these files were controlled and merged, model inputs were calculated based on the Matlab Simulink code with steady-state model input calculation at each time step in transient data. The models were run with quasi-steady assumptions at each time step in transient data in Python. The cumulative fuel going into the oil pan was calculated over each transient cycle separately by summation of oil dilution formation rate at each time step. The fuel concentration in oil was calculated by dividing cumulative fuel volume in oil at the end of the cycle by the sum of cumulated fuel volume and initial oil volume.

In Figure 4.25, transient test and model results were shown together. Again, Y-Axis was limited to a logical value to make the figure more readable.

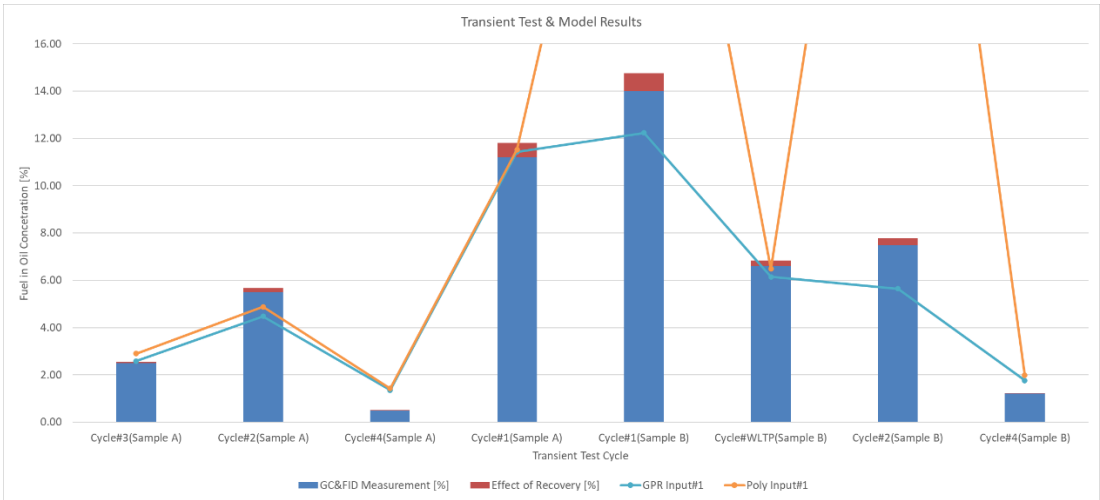

Figure 4.25 : Transient test and model results.

Polynomial regression showed a high deviation in extrapolation, where the Gaussian process kept giving reasonable figures. Gaussian process results were tended to undershoot in the case of Sample B when Cycle#1 and Cycle#2 were considered. In addition to that, Gaussian process results showed overshooting for Cycle# 4 with both Sample A and Sample B.

5. CONCULSION / DISCUSSIONS

In conventional calibration development processes, active DPF regeneration calibration was developed with multiple loops over various transient cycles. Since the measuring oil dilution formation rate of a specific calibration is not possible simultaneously, multiple calibrations shall be prepared and tried out at transient cycles to observe the oil dilution status of these calibrations. The combined effect of several engine control parameters over oil dilution is not possible to foresee directly. Therefore, multiple calibrations to find a local minimum is needed if a modelling approach for oil dilution does not exist. Moreover, the oil dilution status of engine oil is monitored by map-based algorithms. Once the calibration set is selected among multiple calibration iterations, map-based algorithms to estimate the level of oil dilution should be calibrated with individual test results. All of that development process is shown in Figure 5.1.

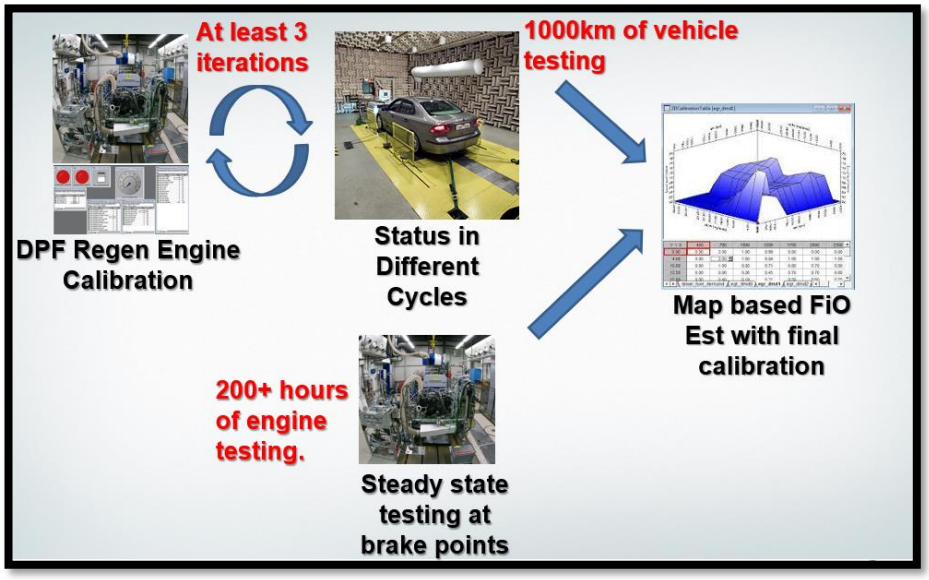

Figure 5.1 : Conventional development process.

In the proposed way of working within the thesis, a Design-of-Experiment is planned to get extensive information on oil dilution formation characteristics of the tested engine similar to steady-state testing performed in the content of this thesis. Once the

Gaussian process model is deployed, the model can be used to assess oil dilution formation metrics of different engine calibrations. Moreover, the Gaussian process model can be used to create a calibration for map-based algorithms to monitor the oil dilution level for the engine calibration picked. As a final stage of the development project, the oil dilution metric of the project can be determined by running transient tests, and the map-based oil dilution model within the ECU can be tuned based on that final dataset. The proposed workflow is shown in Figure 5.2.

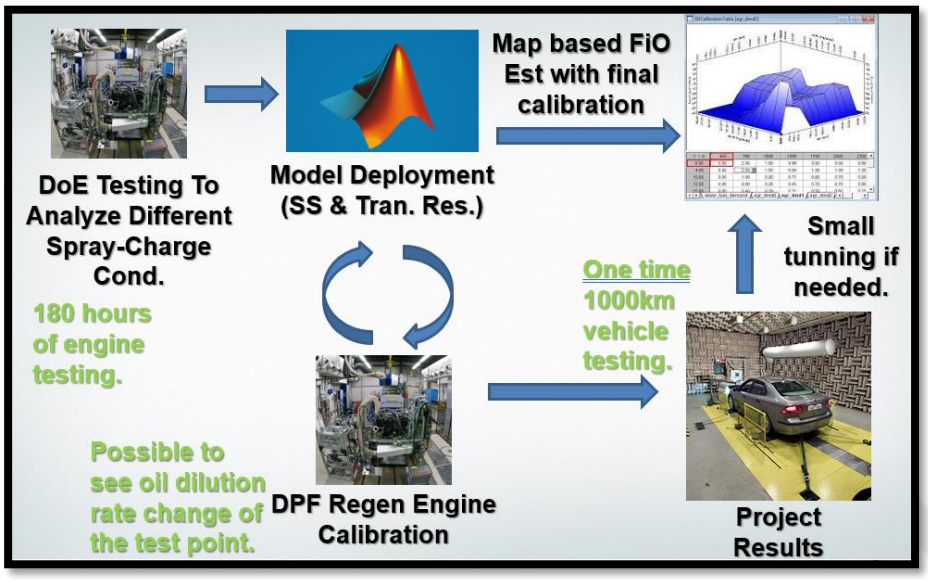

Figure 5.2 : New development process proposal.

- Studies have shown a certain correlation between inputs of SMD, normalized spray penetration depth and engine speed and output of oil dilution rate. By this correlation, the Gaussian process achieved $R^2 = 0.86$ in steady-state conditions. In addition to the Gaussian process, polynomial regression was also applied, and the accuracy of $R^2 = 0.82$ was shown in steady-state.
- According to the engine tests and the oil samples, the studied post injections induced oil dilution. In particular, second post injections in the range of 120 – 150 CA aTDC were showed extremely high oil dilution generation compared to first post injections in the range of 30 – 50 CA aTDC.
- This study showed that oil recovery has asymptotic behaviour. Moreover, exponential expressions can reflect that behaviour as a function of duration and initial heavy/light fraction.

- With statistical approaches, the over-fitting risk of the model should always be checked. Since the statistical models can be flexible enough to memorize the input data, this possibility is avoided by limiting the model flexibility to the point that enough to model input data but not to deviate extremely out of input data. Dividing input data into two fractions, one as test data and one as train data, is beneficial to avoid that risk.
- During the modelling studies, the Pearson coefficient is shown to be helpful to catch correlation between oil dilution and input parameters. Moreover, adding more parameters that have internal correlation resulted in a very high over-fitting risk.
- Polynomial regression showed a high rate of oil dilution formation values in some test points, resulting in relatively high deviations in Cycle#1 and Cycle#2 for Sample B. Therefore, polynomial regression is not acceptable. On the other hand, the Gaussian process did not show that behaviour.
- Cycle#4 had the highest average vehicle speed among all cycles in the transient test matrix. Therefore, Cycle#4 required high power to keep the vehicle at high speed. Thus, the second post-injection quantity demand was low by the temperature controller to keep filter inlet temperature at 600°C. Consequently, models were severely affected by injection accuracy at low injection demands where accuracy was expected to be poor.
- Since the complete test matrix took 304 hours of testing, a level of noise can be expected on test results, although a considerable effort was spent to check and keep the same operating conditions.

REFERENCES

[1] **URL-1** <*https://dieselnet.com/standards/eu/hd.php*>, date retrieved 09.2021.

[2] **Tiexlong Huang, Guangdl Hu, Feng Guo, Yuanxian Zhu** (2019). Investigation of a Model-Based Approach to Estimating Soot Loading Amount in Catalyzed Diesel Particulate Filters, *SAE Technical Paper Series*.

[3] **Ourania Voutsi, Dimitrios Tsinoglou, Dimitrios Karamitros, Grigorios Koltsakis** (2019). Pressure Drop of Particulate Filters and Correlation with the Deposited Soot for Heavy-Duty Engines, *SAE Technical Paper Series*.

[4] **Tormosa B., Novellaa R.,Sorianoa J.,Barberáa A.,Tsujib N.,Ueharab I.,Alonso M.** (2019). Study of the influence of emission control strategies on the soot content and fuel dilution in engine oil, *Tribology International.*

[5] **Madhu Singh, Mek Srilomsak, Yujun Wang, Katsunori Hanamura, Randy Vander Wal** (2018). Nanostructure changes in diesel soot during NO2-O2 oxidation under diesel particulate filter-like conditions toward filter regeneration, *International Journal of Engine Research.*

[6] **Mark Wattrus** (2013). Fuel Property Effects on Oil Dilution in Diesel Engines, *SAE Technical Paper Series.*

[7] **F.Motamen, Salehi A. Morina, A.Neville** (2017). The effect of soot and diesel contamination on wear and friction of engine oil pump, *Tribology International.*

[8] **R.Penchaliah, T.J.Harvey, R.J.K.Wood, K.Nelson and H.E.G.Powrie** (2011). The effect of diesel contaminants on tribological performance on sliding steel on steel contacts, *Proceedings of the Institution of Mechanical Engineers.*

[9] **Gen Shibata, Shogo Nishiuchi, Shuntaro Takai, Yoshimitsu Kobashi, Hiroki Kanbe, Eriko Matsumura** (2017). Fuel adhesion and oil splash on oil-wet cylinder walls with post diesel fuel injections, *International Journal of Engine Research.*

[10] **Todd D Fansler, Mario F Trujillo, Eric W Curtis** (2017). Spray-wall interactions in direct-injection engines: An introductory overview, *International Journal of Engine Research.*

[11] **Christina Artmann, Marcel Kaspar and Hans-Peter Rabl** (2013). A New Measurement Technique for Online Oil Dilution Measurement, *SAE International Journal of Fuels and Lubricants.*

[12] **Kidoguchi Y.,Nada Y., Sangawa S., Kitazaki M., Matsunaga D.** (2018). Effect of low load combustion and emissions on fuel dilution in lubricating oil

and deposit formation of DI diesel engines fueled by straight rapeseed oil, *Fuel.*

[13] **Hulkkonen T., Tilli A., Kaario O., Ranta O., Sarjovaara T., Vuorinen V., Larmi M., Lehto K.** (2018). Late post-injection of biofuel blends in an optical diesel engine: Experimental and theoretical discussion on the inevitable wall-wetting effects on oil dilution, *International Journal of Engine Research.*

[14] **ASTM** (2020). *Standard Test Method for Diesel Fuel Diluent in Used Diesel Engine Oils by Gas Chromatography*.

[15] **URL-2** *<https://www.peakscientific.com/discover/news/how-does-an-fid-work/#:~:text=An%20FID%20uses%20a%20flame,which%20ionises%20the%20carbon%20atoms>*, date retrieved 07.2021.

[16] **Takayuki Ito, Takaaki Kitamura, Hirokazo Kojima, Hiroshi Kawanabe** (2019). Prediction of Oil Dilution by Post-Injection in DPF Regeneration Model, *SAE Technical Paper Series*.

[17] **Hiro Hiroyasu and Masataka Arai** (1990)**.** Structures of Fuel Sprays in Diesel Engines, *SAE Technical Paper Series*.

[18] **Xinyi Zhou, Tie Li, Zheyuan Lai, Yijie Wei** (2019). Modelling Diesel Spray Tip and Tail Penetrations After End-of-Injection, *Fuel*.

[19] **Benjamin Berger, Florian Rauscher and Boris Lohmann** (2011). Analyzing Gaussian Processes for Stationary Black-Box Combustion Engine Modelling, *IFAC World Congress*.

[20] **Tobias Gutjahr, Holger Kleinegraeber, Thorsten Huber and Thomas Kruse** (2015). Advanced Statistical System Identification in ECU-Development and Optimization, *SAE International*.

[21] **Benjamin Berger and Florian Rauscher** (2012). Robust Gaussian Process Modelling For Engine Calibration, *Mathematical Modelling Conference*.

CURRICULUM VITAE

Name Surname **:** Murat Gönül

EDUCATION **:**

- **B.Sc.** **:** 2010, Istanbul University, Mech.Eng.
- **M.Sc.** **:** 2015, Istanbul Technical University, Mech.Eng.

PROFESSIONAL EXPERIENCE AND REWARDS:

- 2012-2020 Ford Otosan, Technical Specialist
- 2020-… DAF Trucks, Senior Software Eng.

PUBLICATIONS, PRESENTATIONS AND PATENTS ON THE THESIS:

- **Murat G.,** O.Akın K., A.Tolga Ç., F.Orçun P., 2021: Prediction of Oil Dilution Formation Rate Due to Post Injections in Diesel Engines by Gaussian Process, Fuel.(Publication)
- **Murat G.,** O.Akın K., A.Tolga Ç., 2020: Prediction of Oil Dilution Formation Rate Due to Post Injections in Diesel Engines by Gaussian Process, INCOS.(Conference proceding)